Scaling of shoot and root respiration rate, fresh mass, and surface area of *Fagus crenata* during ontogeny

Yoko Kurosawa

2022

Thesis organization

This thesis investigates the scaling of respiration, fresh mass, and surface area of *Fagus crenata* throughout ontogeny and consists of two chapters.

Chapter 1 shows the size scaling of respiration rate, fresh mass, and surface area of leaves, stems, and roots in seedlings of current year to 1-year old. The chapter discusses how seedlings survive the first year after germination, when mortality is especially high.

Chapter 2 shows the scaling of respiration, fresh mass, and surface area in shoot and root from germinating seeds to mature trees. This chapter focuses on the zero-sum relationship between shoot and root and discusses the role of the root system during the entire ontogeny of individual trees.

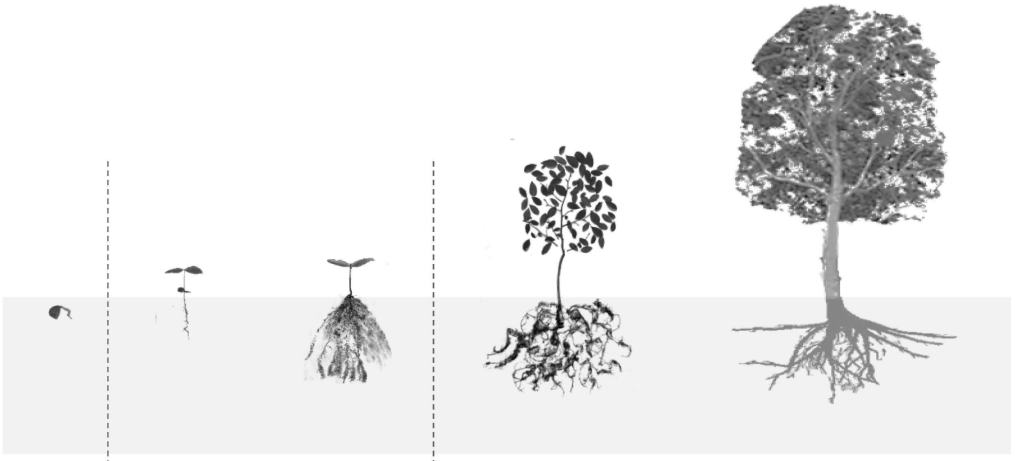

Contents

Figures

Tables

Chapter 1

Scaling of fresh mass, surface area, and respiration of leaves, stems, and roots of *Fagus crenata* seedlings from current-year to 1-year old

As terrestrial plants are rooted in one place, their metabolism must be acclimatized to continuously changing environmental conditions. This process is influenced by different metabolic traits of plant organs during ontogeny. However, direct measurement of organ-specific metabolic rates is particularly scarce, and little is known about their roles in whole-plant metabolism. In this study, we investigated size scaling of respiration rate, fresh mass, and surface area of leaves, stems, and roots in 65 seedlings of *Fagus crenata* Blume (2 weeks to 16 months old). With the increase in plant mass, a proportion of roots in whole plant increased from 20.8 to 87.3% in fresh mass and from 12.8 to 95.0% in surface area, while only from 15.6 to 60.2% in respiration rate. As a result, the fresh-mass- and surface-area-specific respiration rates in the roots decreased by 85% and 90%, respectively, and these decreases were significantly size-dependent. However, such a size-dependent decrease was not observed for the surface-area-specific respiration rate in the leaves and stems. It is likely that this rapid root development is specific to the early growth stage after germination and would help plants acquire water and nutrients efficiently (i.e., at relatively low respiratory carbon costs). Overall, it is probable that the establishment of *F. crenata* forests and survival of *F. crenata* seedlings could be promoted by substantial root growth with a reduction in respiratory carbon cost.

1. Introduction

Metabolism, which includes various fundamental biological processes that transform energy and materials, helps organisms to adapt to changing environmental conditions [1,2]. Therefore, the metabolic rate has profound physiological, ecological, and evolutionary implications [3,4], and it could be key for understanding and predicting the effects of climate change on individuals and ecosystems [1,2].

In general, the metabolic rate of an organism (i.e., the respiration rate, R) scales with body size. In order to obtain a mechanistic insight into the regulation of metabolic rate scaling, empirical evidence should be gathered from whole-organism measurements [5]. The scaling of metabolic rate is usually described as a simple power function of body mass (X):

$$R = aX^b \quad (1)$$

where, a is the normalization constant and b is the scaling exponent (slope on the log–log coordinates) [6–8]. Equation (1) represents the metabolic rate as a function of body size under different environmental and phylogenetic constraints [2,5,8–11]. To date, most studies on the regulation of metabolic scaling were based on indirect evidence and were aimed at constructing theoretical models to explain the scaling exponent b, which has been widely assumed to be 3/4 according to the WBE model [5–8,12,13]. From a metabolic perspective, using fresh mass as the proxy for body size (X) is important because all active components (such as enzymes) are contained in the liquid phase, and they are the ultimate sources of energy for metabolic activities [14,15]. In evolutionary biology, comparisons of metabolic scaling among various taxa, such as prokaryotes, animals, algae, and vascular plants, have been performed using fresh mass as a proxy for individual body size [9,16]. In this context, an empirical study with direct evidence on the metabolic rate and fresh mass of individual organisms could increase our understanding of the regulation of metabolic scaling.

To study the scaling of metabolic rate of individual organisms, it is important to understand the size scaling of organ respiration. This is because individual organisms are complex systems that depend on the integrated performance of various organ structures and their functions [4,17]. In plants, biomass allocation to the leaves, stems (including the main stems and branches), and roots must be balanced for their growth [18–21], and the root/shoot biomass ratio likely changes during ontogeny and shows size dependency as a consequence of allometric, physiological, and ontogenetic conditions in plant evolution [23–30]. Therefore, metabolic scaling in plants involves size-dependent allocation of fresh mass, surface area, and respiration rate among organs in individual plants. However, there are only a few empirical studies on the size scaling of allocation of energy, that is, the distribution of respiration rate among organs in individual plants [31].

Fagus is one of the most widespread and dominant genera in temperate deciduous broadleaf forests in the circumpolar Northern Hemisphere [32], and the species of this genus are relatively drought sensitive [33–35]. *Fagus crenata* Blume is one of the most typical canopy tree species of cool temperate forests that is widely distributed across Japan [36,37]. Pure *F. crenata* forests are often established in snowy areas along the Japan Sea [38]. During the first year after germination, *F. crenata* seedlings have a high mortality rate because of various environmental factors, such as drought stress, insufficient light, and fungal pathogens [39–41]. Thus, this period is considered as the bottleneck phase in the population. To date, little is known about the whole-plant physiology of *F. crenata* seedlings in this phase.

In this study, we assessed the size scaling of fresh mass, surface area, and respiration rate in the leaves, stems, and roots of 65 *F. crenata* seedlings (2 weeks to 16 months old). We assumed that the size-dependent shifts in fresh mass, surface area, and respiration rate among plant organs in a certain growth stage represent fundamental adaptations for that growth stage. Based on this assumption, we hypothesized that there is a size-dependent shift in the allocation of fresh mass, surface area, and

respiration rate that is specific to the early growth stage, which is characterized by high mortality. To test this hypothesis, we also assessed the root/shoot ratio of fresh mass in various plant growth stages, from seedling to mature tree stages, using the data from our previous studies [5,42]. Testing our hypothesis could help to understand how seedlings survive the first year after germination when mortality is especially high and help describe the population dynamics of *F. crenata*.

Previous studies have revealed the geographical variation of *F. crenata*, mainly for above-ground parts, such as morphological and physiological traits of leaves [37,43,44]. However, despite the importance of root for individual plant growth, these studies have rarely focused on roots. Therefore, the understanding of the ontogenetic change in shoot and root respiration at the whole-plant level in *F. crenata* seedlings would help advance our understanding of their ecophysiological responses in relation to population dynamics in the bottleneck phase at the local environment. In this study, we used *F. crenata* seedlings of one of the most typical snowy regions in Japan, where we focused on one haplotype of *F. crenata* and investigated the ecological significance of ontogenetic change in root and whole-plant respiration. Ultimately, the understanding of the geographic variation in respiration rate at the whole-plant and organ-level, which is expected to be related to differences in the amount of snowfall in winter, would help to interpret the geographic differences in physiological traits as adaptations to various local environment.

2. Materials and Methods

(a) Ethics statement

Our fieldwork included collection of *F. crenata* seeds in a Japanese national forest in the city of Tsuruoka. The fieldwork was permitted by the Shonai District Forest Office, and did not involve any endangered or protected species.

(b) Plant material and experimental design

In October 2013 and 2015, we collected seeds from trees in a mature forest of *F. crenata* in Tsuruoka, Yamagata prefecture (38°32′N, 139°56′E), and sowed them in December in both years. This forest is one of the most representative *F. crenata* forests along the Japan Sea; therefore, the collected seeds belong to the haplotype prevalent on the Japan Sea coast [36,45]. The seeds collected in 2013 germinated in mid-April 2014 and those collected in 2015 germinated in mid-April 2016, and almost all the germinated seedlings were healthy. In late April of 2014 and 2016, we transplanted approximately 100 two-week-old healthy seedlings to 0.9 L pots and placed them under natural light conditions outside the Yamagata University Tsuruoka Campus (38°44′N, 139°49′E). The pots were filled with a mixture of commercially available leaf mold (Hirota Shoten Co. Ltd., Tochigi, Japan) and Kanuma pumice (Tachikawa-Heiwa Nouen Co. Ltd., Tochigi, Japan), which retains moisture and allows air permeability in the soil. The monthly mean temperature in Tsuruoka ranged from 1.9°C in January to 25.1°C in August (an annual mean of 13.6°C) in 2015 and from 2.2°C in January to 26.4°C in August (an annual mean of 13.5°C) in 2016. The annual precipitation was 1556 mm in 2015 and 1992 mm in 2016. We watered the pots well every day for 20 days after germination; thereafter, we only watered them on days of insufficient rain. During the experiment, almost all the seedlings including those were transplanted to pots and those were not transplanted remained healthy, and none of them died.

We conducted 12 measurement campaigns in the period from 2015 to 2016. In each measurement, we harvested 4–6 seedlings that were grown in pots and measured the fresh mass (kg), surface area (m^2), and respiration rate (μmol CO_2 s^{-1}) of their roots, stems, and leaves. In 2015, the measurements were conducted two times in August, using 15- to 16-month-old seedlings that germinated in mid-April 2014. In 2016, the measurements were conducted two times at 2- or 3-week intervals every month from early May to early September using 2-week to 5-month-old seedlings

that germinated in mid-April 2016. These seedlings were selected to represent the widest possible range of seedling growth stages. The total number of harvested and measured seedlings was 65 and the whole-plant fresh mass ranged from 41.2×10^{-5} to 23.5×10^{-3} kg (table 1.1).

Table 1.1 Minimum and maximum values of fresh mass, surface area, and respiration of whole plant, roots, leaves, and stems at the individual level among all seedlings (n = 65).

	Fresh mass ($\times 10^{-5}$ kg)		Surface area ($\times 10^{-4}$ m^2)		Respiration rate ($\times 10^{-4}$ μmol CO_2 s^{-1})	
	Min.–Max.	Max./Min.	Min.–Max.	Max./Min.	Min.–Max.	Max./Min.
Whole plant	41.2–2350.0	57.0	23.6–1210.0	51.3	8.7–131.0	15.1
Roots	7.0–1730.0	247.1	2.5–998.0	399.2	0.8–52.6	65.8
Leaves	19.3–172.0	8.9	19.2–185.0	9.6	4.6–53.3	11.6
Stems	8.5–480.0	56.5	1.4–32.9	23.5	1.1–42.3	38.5

(c) Measurement of respiration rate and surface area

Respiration rate was measured following the method developed by Mori et al. (2010). Immediately after excision, the plants were ssprayed with water and the respiration rate was measured within 20 min; the plant material was wrapped in wet paper to prevent transpiration. Following the guidance of previous studies on organ respiration rate [46–48], soil particles adhering to the roots were removed by washing. Subsequently, the plants were separated into roots, stems, and leaves. These washing and separation processes did not have any effect on the measured values of whole-plant respiration rate, as reported by Mori et al. (2010) [5]. Different plant organs were placed in custom-made aluminum chambers (80 or 160 cm^3) that were impenetrable to light. The CO_2 concentration within the chamber was measured every 5 s for approximately 30–300 s using an infrared CO_2 analyzer (GMP343; Vaisala, Helsinki, Finland) and normalized to 20°C under the assumption that $Q_{10} = 2$. The variation in temperature within the chambers during the measurements was at most 1°C.

Leaf surface area was measured using a leaf area meter (LI-3100C; LICOR, Lincoln, NE, USA). Stem surface area was calculated as the sum of the surface area of stem and branch sections from their diameter and length, assuming that the stem and branches were cylindrical. Root surface area was determined using image analysis software WinRhizo version 2016a (Regent Instruments, Quebec, Canada). Root images for analysis were obtained using a flatbed scanner (Epson Perfection V800, Seiko Epson, Japan) at the resolution of 800 dpi.

(d) Data analysis

Scaling relationships were analyzed using a simple power function on log–log coordinates based on reduced major axis (RMA) regression [49] of the log-transformed version of equation (1), (for

all analyses, $n = 65$) using PAST statistical software [50]. We assessed the scaling of respiration rate vs. fresh mass and surface area for the whole plant and leaves, stems, and roots. For each plant organ, we also assessed the scaling of surface area vs. fresh mass, and fresh-mass- and surface-area-specific respiration rate vs. whole-plant fresh mass. Finally, we assessed the scaling of root/shoot ratio of fresh mass, surface area, and respiration rates vs. whole-plant fresh mass. In addition, we assessed fresh-mass-based root/shoot ratio from our previous research, ranging from current-year of germination to approximately 80 years of age ($n = 264$) [5,42], with that of the 65 seedlings.

These regression analyses were conducted with fresh mass as a proxy for body size or organ size following the methods described by previous studies [5,16]. As a proxy for size scaling, fresh mass would better reflect physiological properties of organs than dry mass [14,15]. Mori et al. (2010)[5], who directly measured whole-plant respiration of trees ranging from small seedlings to large trees, also used fresh mass as a proxy for body size to analyze the size scaling of whole-plant respiration rate. Our statistical inference to compare the scaling exponents was based on the 95% confidence interval (CI). In the case of no overlap among 95% CIs between groups, the differences among them were significant.

3. Results

(a) Size scaling of respiration and surface area

Size scaling of whole-plant respiration rate vs. whole-plant fresh mass and whole-plant respiration vs. whole-plant surface area showed significantly negative allometry (i.e., $b < 1$). There was no significant difference in the exponents between these relationships at the 95% CI level (figure 1.1*a*, *b*, table 1.2).

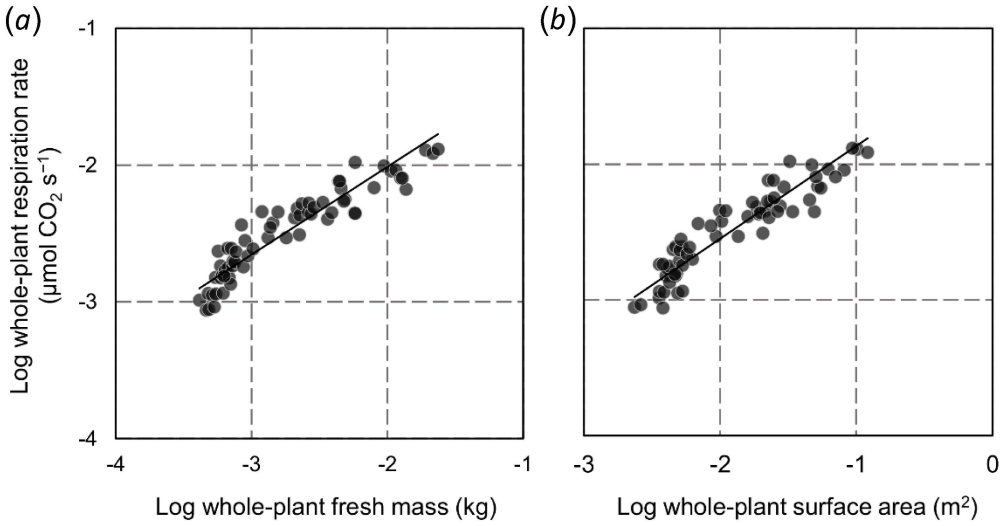

Figure 1.1 Results of the reduced major axis (RMA) analysis showing the relationships between whole-plant respiration and (*a*) whole-plant fresh mass and (*b*) whole-plant surface area. In each analysis, $n = 65$.

The roots showed a wider range of variation in surface area (393-fold, table 1.1) than that in fresh mass (246-fold). As shown in figure 1.2, the scaling of root surface area vs. root fresh mass was significantly positive (i.e., $b > 1$) at the 95% CI level. Compared with the variation in root surface area and root fresh mass, the variation in root respiration rate (65.8-fold) presented a narrow range. As a result, the scaling of root respiration rate vs. root surface area and root respiration rate vs. root fresh mass was allometrically negative (i.e., $b < 1$). The scaling exponent of root respiration vs. root surface area was lower than that of root respiration vs. root fresh mass, although the difference was not significant at the 95% CI level (figure 1.3*a*, *b*, table 1.2).

The leaves showed a similar range of variation in surface area (9.64-fold, table 1.1) and fresh mass (8.91-fold), resulting in nearly isometric scaling (i.e., $b = 1$) for leaf area vs. leaf fresh mass (figure 1.2). Furthermore, the variations in surface area and fresh mass were close to those in respiration rate (11.6-fold). We found isometric exponents for the scaling of leaf respiration rate vs. leaf area, and leaf respiration rate vs. leaf fresh mass (figure 1.3*a*, *b*, table 1.2).

The stems showed a wider range of variation in fresh mass (56.3-fold, table 1.1) than that in surface area (23.0-fold), revealing a negative allometry of stem surface area vs. stem fresh mass (figure 1.2). The range of variation in stem respiration rate (38.5-fold) was narrower than that in stem fresh mass, but wider than that in stem surface area. Consequently, the scaling of stem respiration rate vs. stem surface area was nearly isometric, whereas the scaling of stem respiration vs. stem fresh mass was allometrically negative (figure 1.3*a*, *b*, table 1.2).

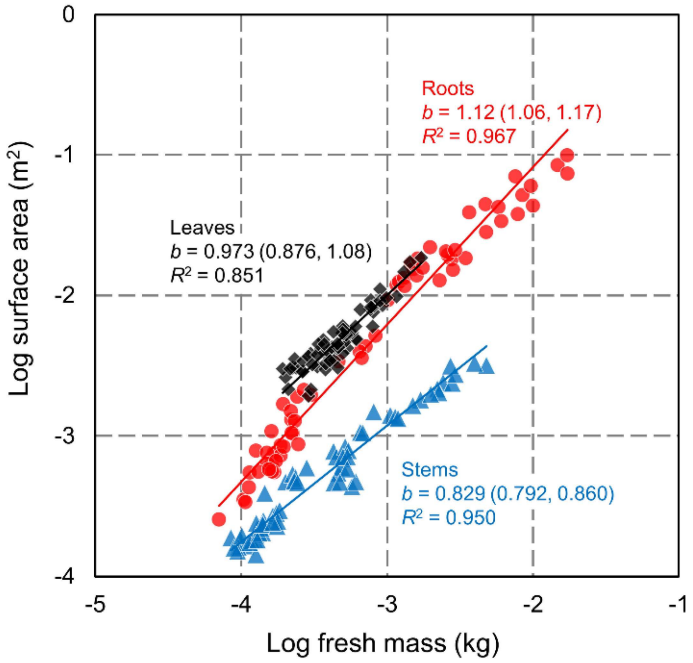

Figure 1.2 Results of the reduced major axis (RMA) analysis showing the relationships between surface areas and fresh mass of different plant organs. Black diamonds represent total leaves, blue triangles represent total stems, and red circles represent total roots of individual seedlings. In each analysis, n = 65. The value in parentheses is 95% CI of exponent b.

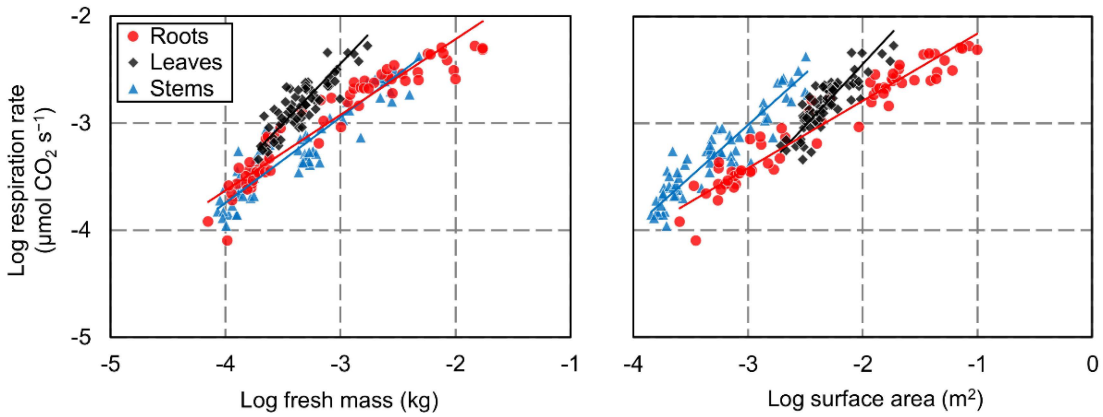

Figure 1.3 Results of the reduced major axis (RMA) analysis showing the relationships between respiration and (*a*) fresh mass and (*b*) surface area in different plant organs. Black diamonds represent total leaves, blue triangles represent total stems, and red circles represent total roots of individual seedlings. In each analysis, $n = 65$. Details are compiled in table 1.2.

Table 1.2 Results of reduced major axis (RMA) regression showing the relationships among respiration, fresh mass, and surface area of whole plant, roots, leaves, and stems.

	Exponent (b)	95% CI of b	Normalization constant (a)	95% CI of a	R^2
Respiration rate vs. fresh mass					
Whole plant	0.642	0.576–0.699	0.1870	0.1190–0.2660	0.869
Roots	0.706	0.637–0.767	0.1570	0.0928–0.2400	0.901
Leaves	1.120	0.990–1.250	8.2800	2.9300–21.6000	0.730
Stems	0.799	0.736–0.868	0.2840	0.1660–0.4950	0.833
Respiration rate vs. surface area					
Whole plant	0.685	0.620–0.743	0.0660	0.0485–0.0850	0.868
Roots	0.630	0.587–0.672	0.0295	0.0232–0.0365	0.929
Leaves	1.150	0.962–1.300	0.7190	0.2510–1.6000	0.722
Stems	0.964	0.886–1.050	0.7530	0.4080–1.4200	0.867

In all regressions, $n = 65$ and $p < 0.001$.

(b) Fresh-mass- and surface-area-specific respiration rates of plant organs

The results of the analysis of scaling of fresh-mass- and surface-area-specific respiration rate in different plant organs vs. whole-plant fresh mass are shown in figure 1.4*a*, *b* and table 1.3. Among the three organs, the roots showed the steepest decrease in both fresh-mass-specific respiration rate and surface-area-specific respiration rate, and this decrease was significantly size dependent. Conversely, for leaves, both fresh-mass-specific respiration rate and surface-area-specific respiration rate did not significantly change with the increase in plant size. Finally, for stems, both fresh-mass-specific respiration rate and surface-area-specific respiration rate showed a decrease with an increase in plant size; however, compared with the decrease in the fresh-mass-specific respiration rate, the decrease in surface-area-specific respiration rate was not significantly size-dependent.

The exponent for the surface-area-specific respiration rate in the roots was significantly lower than that in the leaves and stems at the 95% CI level. On the regression line, with the increase in whole-plant fresh mass, the surface-area-specific root respiration rate declined by approximately 90% (from 0.507 to 0.0496 μmol CO_2 s^{-1} m^{-2}), and the fresh-mass-specific root respiration rate declined by approximately 85% (from 2.6 to 0.387 μmol CO_2 s^{-1} kg^{-1}). In addition, among the three organs, the size-dependent decrease in surface-area-specific respiration rate was observed only in the roots. These results indicate that only the roots exhibited a significant decrease in respiratory carbon cost on a surface-area basis and fresh-mass basis with the increase in plant mass.

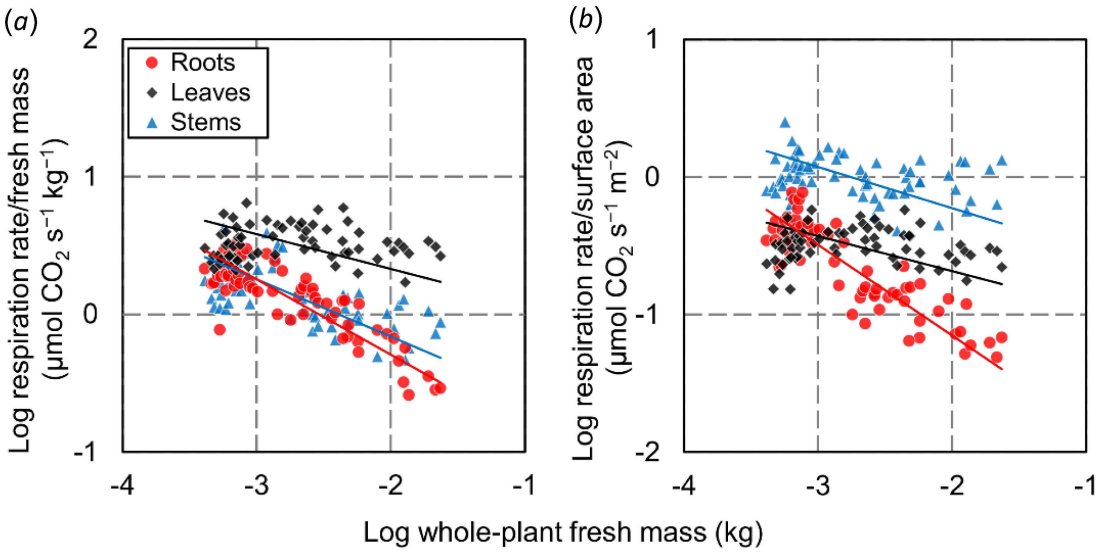

Figure 1.4 Results of the reduced major axis (RMA) analysis showing the relationships between (*a*) fresh-mass-specific respiration rate and (*b*) surface-area-specific respiration rate of plant organs in relation to whole-plant fresh mass. Black diamonds represent total leaves, blue triangles represent total stems, and red circles represent total roots of individual seedlings. In each analysis, $n = 65$. Details are compiled in Table 1.3.

Table 1.3 Results of reduced major axis (RMA) regression: scaling of fresh-mass-specific respiration rate (μmol CO_2 s^{-1} kg^{-1}) and surface-area-specific respiration rate (μmol CO_2 s^{-1} m^{-2}) in the roots, leaves, and stems with whole-plant fresh mass (kg).

	Exponent (*b*)	95% CI of *b*	Normalization constant (*a*)	95% CI of *a*	R^2	*p*
Fresh-mass-specific respiration rate vs. whole-plant fresh mass						
Roots	−0.548	−0.608 to −0.489	0.0408	0.0275–0.0585	0.739	< 0.001
Leaves	−0.252	−0.807 to −0.207	0.6700	0.0189–0.8910	0.001	0.811
Stems	−0.417	−0.497 to −0.335	0.1010	0.0624–0.1730	0.414	< 0.001
Surface-area-specific respiration rate vs. whole-plant fresh mass						
Roots	−0.659	−0.733 to −0.575	0.0034	0.0021–0.0057	0.763	< 0.001
Leaves	−0.255	−0.823 to −0.215	0.0638	0.0017–0.0833	0.003	0.647
Stems	−0.299	−0.373 to −0.230	0.1500	0.0911–0.2430	0.067	0.037

In all regressions, $n = 65$.

(c) Ontogenetic shift in the root/shoot ratio

As shown in figure 1.5, slope *b* for the scaling of root/shoot ratio of surface area was significantly larger than that of fresh mass and respiration rate at the 95% CI level. In addition, there was no significant difference between slope *b* for the scaling of root/shoot ratio of fresh mass and that of respiration rate. Slope *b* of root/shoot ratio was 1.19 for surface area (95% CI: 1.01–1.34, R^2 = 0.748), 0.807 for fresh mass (95% CI: 0.689–0.910, R^2 = 0.756), and 0.637 for respiration rate (95% CI: 0.492–0.754, R^2 = 0.447). From the smallest to the largest studied plants, the root/shoot ratio on these regression lines increased from 0.146 to 18.9 for the surface area (12.8 to 95.0% in whole-plant surface area), 0.263 to 6.88 for fresh mass (20.8 to 87.3% in whole-plant fresh mass), and 0.184 to 1.51 for respiration rate (15.6 to 60.2% in whole-plant respiration rate).

Therefore, the roots showed not only the largest decrease in fresh-mass- and surface-area-specific respiration rates (figure 1.4*a*, *b*), but also the largest increase in fresh mass and surface area among the three organs. These results revealed that the negative allometry of whole-plant respiration rate (figure 1.1*a*, *b*) was caused by the increase in the proportion of roots in whole-plant fresh mass and surface area, as well as by the decrease in fresh-mass- and surface-area-specific root respiration with the increase in plant size.

In a greater plant mass over the 65 measured seedlings, the root/shoot ratio showed a gradual decrease with the increase in whole-plant fresh mass to approximately 0.1–0.3 (10–20% of the whole-plant fresh mass around 10–1000 kg). This indicates that the observed size-related increase in the root/shoot ratio is specific to the seedling stages.

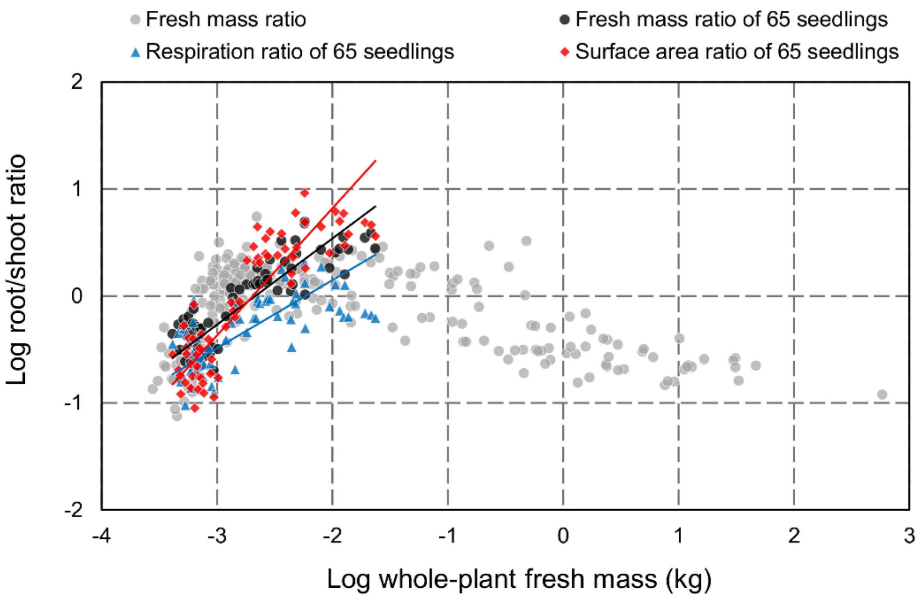

Figure 1.5 Plot diagram of the root/shoot ratios and whole-plant fresh mass of *Fagus crenata* from germination to mature tree stages. Black circles, red diamonds, and blue triangles represent the root/shoot ratio of fresh mass, surface area, and respiration rate, respectively, in the 65 seedlings shown in Figures 1.1–1.4. For these values, regression lines were obtained using the RMA regression analysis (each analysis, $n = 65$ and $p < 0.001$). Gray circles represent the root/shoot ratio of fresh mass obtained from our previous studies ($n = 264$).

4. Discussion

In this study, to the best of our knowledge, we showed for the first time that *F. crenata* seedlings rapidly increase the root surface area available for water and nutrient absorption, and decrease respiratory carbon costs in roots, which are apparent in the decrease in surface-area-specific root respiration rate (figure 1.4*b*). Considering the decrease in fresh-mass root/shoot ratio in plants with a higher whole-plant fresh mass (figure 1.5), the rapid root development with a reduction in respiratory carbon costs is probably specific to the early growth stage of *F. crenata*. Root growth has been suggested to be important for seedlings to avoid nutrient and water deficiency [51,52]. The increase in mass allocation to the shoots after the early growth stage must be preceded by an increase in water and nutrient absorption via the root surface [52]. Therefore, the initial burst of root growth may be an important step to increase photosynthetic performance and consequently accelerate shoot growth. Conversely, failure to achieve a high root/shoot ratio may be one of the physiological factors in seedling death.

In the present study, the mass root/shoot ratio of 4–5-month-old *F. crenata* (between 23.4×10^{-4} and 57.7×10^{-4} kg in whole-plant fresh mass) was 1.07–2.22 (51.7–68.9% in whole-plant fresh mass) on the regression line in our analysis of the size scaling of mass root/shoot ratio. Similar trends were observed by Peuke et al. (2002)[34] in *Fagus sylvatica* L. In their study, the mass root/shoot ratio of 4–5-month-old *F. sylvatica* seedlings was approximately 0.71–1.11 (41.5–52.6% for whole-plant mass) in 10 provenances, which differed in annual precipitation. Therefore, rapid root growth in the early growth stages probably helps successful seedling establishment for not only *F. crenata*, but also other *Fagus* species. The high allocation of biomass to the roots is an important trait of shade-tolerant species, including *F. crenata*. Shade-tolerant species typically exhibit a higher mass root/shoot ratio than shade-intolerant species [53]. The high biomass allocation to the roots is important to defend the seedlings of shade-tolerant

species against multiple hazardous factors, such as herbivores and pathogens, in the understory with low light availability [54]. Therefore, our findings on root development in *F. crenata* are in accordance with the expected survival strategies of shade-tolerant species.

In the early growth stages of the plants assessed in the present study (between 41.2×10^{-5} and 23.5×10^{-3} kg in whole-plant fresh mass), a large proportion of energy (respiration rate) and biomass (fresh mass and surface area) was allocated to the roots as whole-plant fresh mass increased (figure 1.5). However, after the early growth stages, as biomass allocation to the shoots increased with the increase in plant mass, energy allocation to the shoots is expected to increase. This change in preferential energy allocation to the shoots after the early growth stage may cause a gradual increase in photosynthetic performance and growth, as demonstrated by previous studies [55–57].

Several studies in various organisms have suggested that the negative allometry of the metabolic rate is partially due to the increase in the relative masses of organs with low metabolic rates [5,17,58]. One of the reasons for this size-dependent shift is physico–chemical constraints [5,58,59], mainly gravity, which becomes increasingly important as plants grow [60]. However, in a wide range of plants sizes, from seedlings to mature trees, size scaling of root respiration rate remains unclear, even after considering the importance of root system acquisition in the evolution of terrestrial plants [61,62]. In the present study, the negative allometry of whole-plant respiration was due to the increase in the proportion of roots in whole-plant fresh mass and surface area, and the decrease in fresh-mass- and surface-area-specific root respiration with the increase in plant size. These results emphasized that the roots impose major constraints on the scaling of whole-plant respiration rate.

The mechanism by which fresh-mass- and surface-area-specific root respiration rates decreased with the increase in root fraction remains unclear. Considering that the entire root

system consists of roots of different ages, structures, and functions [63,64], more extensive measurements of respiration within different parts of the root system are needed to reveal the mechanism. To date, respiration rate of the entire root system in mature trees has been rarely measured, and scaling relationships of function between individual roots and the entire root systems are not as well established as those between leaf and whole above-ground parts [65]. In our future studies, we need investigate whether the scaling of shoots and root respiration rates of *F. crenata* at the whole-plant level differ among different regions. As to whole-plant respiration rates that include shoots and roots, Mori et al. (2010) [5] and Reich, Tjoelker, Machado, and Oleksyn (2006) [66] have empirically observed that the whole-plant respiration rates would likely be unaffected by growth conditions and would be similar within and among species. Therefore, understanding the scaling of whole-plant respiration, including shoots and roots from seedlings to mature trees within species, would provide insight into the adaptive significance to attain a larger body size irrespective of differences in local environmental conditions. Ultimately, studying the scaling of physiological traits of root and shoot at the whole-plant level in various regions within species would help advance our understanding of the geographic differences at the organ-level as an adaptation of the species to various local environments.

References

1. Brown JH, Gillooly JF, Allen AP, Savage VM, West GB. 2004 Toward a metabolic theory of ecology. *Ecology* **85**, 1771–1789.
2. Sibly RM, Brown JH, Kodric-Brown A. 2012 *Metabolic ecology: a scaling approach*. John Wiley& Sons, Chichester.
3. Enquist BJ, Tiffney BH, Niklas KJ. 2007 Metabolic Scaling and the Evolutionary Dynamics of Plant Size, Form, and Diversity: Toward a Synthesis of Ecology, Evolution, and Paleontology. *Int. J. Plant Sci.* **168**, 729–749.
4. Glazier DS. 2015 Is metabolic rate a universal 'pacemaker' for biological processes? *Biol. Rev.* **90**, 377–407.
5. Mori S *et al.* 2010 Mixed-power scaling of whole-plant respiration from seedlings to giant trees. *Proc. Natl. Acad. Sci. USA.* **107**, 1447–1451.
6. DeLong JP, Okie JG, Moses ME, Sibly RM, Brown JH. 2010 Shifts in metabolic scaling, production, and efficiency across major evolutionary transitions of life. *Proc. Natl. Acad. Sci.* **107**, 12941–12945.
7. Kleiber M. 1932 Body size and metabolism. *Hilgardia* **6**, 315–353.
8. West GB, Brown JH, Enquist BJ. 1997 A general model for the origin of allometric scaling laws in biology. *Science*. **276**, 122–126.
9. Banavar JR, Cooke TJ, Rinaldo A, Maritan A. 2014 Form, function, and evolution of living organisms. *Proc. Natl. Acad. Sci. USA.* **111**, 3332–3337.
10. Glazier DS. 2018 Rediscovering and reviving old observations and explanations of metabolic scaling in living systems. *Systems* **6**, 4.
11. Yagi M, Kanda T, Takeda T, Ishimatsu A, Oikawa S. 2010 Ontogenetic phase shifts in metabolism: links to development and anti-predator adaptation. *Proc. Biol. Sci.* **277**, 2793–2801.
12. Dodds PS, Rothman DH, Weitz JS. 2001 Re-examination of the "3/4-law" of metabolism. *J. Theor. Biol.* **209**, 9–27.
13. Kooijman, S. A. L. M. (2010). *Dynamic energy budget theory for metabolic organisation. Cambridge*: Cambridge University Press.

14. Huang W, Ratkowsky DA, Hui C, Wang P, Su J, Shi P. 2019 Leaf fresh weight versus dry weight: Which is better for describing the scaling relationship between leaf biomass and leaf area for broad-leaved plants? *Forests* **10**, 256.

15. Thakur D, Rathore N, Chawla A. 2019 Increase in light interception cost and metabolic mass component of leaves are coupled for efficient resource use in the high altitude vegetation. *Oikos* **128**, 254–263.

16. Makarieva AM, Gorshkov VG, Li B-L, Chown SL, Reich PB, Gavrilov VM. 2008 Mean mass-specific metabolic rates are strikingly similar across life's major domains: Evidence for life's metabolic optimum. *Proc. Natl. Acad. Sci. USA.* **105**, 16994–16999.

17. Oikawa S, Itazawa Y. 2003 Relationship between summated tissue respiration and body size in a marine teleost, the porgy *Pagrus major*. *Fish. Sci.* **69**, 687–694.

18. Bloom AJ, Chapin FS, Mooney HA. 1985 Resource limitation in plants resource limitation in plants – an economic analogy. *Annu. Rev. Ecol. Syst.* **16**, 363–392.

19. Ferrio JP, Kurosawa Y, Wang M, Mori S. 2018 Hydraulic constraints to whole-tree water use and respiration in young *Cryptomeria* trees under competition. *Forests* **9**, 449.

20. Franklin O, Johansson J, Dewar RC, Dieckmann U, McMurtrie RE, Brännström AK, Dybzinski R. 2012 Modeling carbon allocation in trees: A search for principles. *Tree Physiol.* **32**, 648–666.

21. Niklas KJ, Enquist BJ. 2002 Canonical rules for plant organ biomass partitioning and annual allocation. *Am. J. Bot.* **89**, 812–819.

22. Shipley B, Meziane D. 2002 The balanced-growth hypothesis and the allometry of leaf and root biomass allocation. *Funct. Ecol.* **16**, 326–331.

23. Ackerly DD, Dudley SA, Sultan SE, Schmitt J, Coleman JS. 2000 The evolution of plant ecophysiological traits: Recent advances and future directions. *Bioscience* **50**, 979–995.

24. Enquist BJ, Niklas KJ. 2002 Global allocation rules for patterns of biomass partitioning in seed plants. *Science.* **295**, 1517–1520.

25. Gedroc JJ, McConnaughay KDM, Coleman JS. 1996 Plasticity in root/shoot partitioning: optimal, ontogenetic, or both? *Funct. Ecol.* **10**, 44–50.

26. Iwasa Y, Jonathan R. 1984 Shoot/root balance of plants: optimal growth of a system with many vegetative organs. *Theor. Popul. Biol.* **25**, 78–105.

27. Ledo A *et al.* 2018 Tree size and climatic water deficit control root to shoot ratio in individual trees globally. *New Phytol.* **217**, 8–11.

28. McConnaughay KDM, Coleman JS. 1999 Biomass allocation in plants : ontogeny or optimality ? a test along three resourcegradients. *Ecology* **80**, 2581–2593.

29. Modrzyński J, Chmura DJ, Tjoelker MG, Thomas S. 2015 Seedling growth and biomass allocation in relation to leaf habit and shade tolerance among 10 temperate tree species. *Tree Physiol.* **35**, 879–893.

30. Poorter H, Niklas KJ, Reich PB, Oleksyn J, Poot P, Mommer L. 2012 Biomass allocation to leaves, stems and roots: meta-analysis of interspecific variation and environmental control. *New Phytol.* **193**, 30–50.

31. Kong D, Fridley JD. 2019 Does plant biomass partitioning reflect energetic investments in carbon and nutrient foraging? *Funct. Ecol.* **33**, 1627–1637.

32. Fang J, Lechowicz MJ. 2006 Climatic limits for the present distribution of beech (*Fagus* L.) species in the world. *J. Biogeogr.* **33**, 1804–1819.

33. Bolte A *et al.* 2016 Desiccation and Mortality Dynamics in Seedlings of Different European Beech *(Fagus sylvatica* L.) Populations under Extreme Drought Conditions. *Front. Plant Sci.* **7**, 751.

34. Peuke AD, Schraml C, Hartung W, Rennenberg H. 2002 Identification of drought-sensitive beech ecotypes by physiological parameters. *New Phytol.* **154**, 373–387.

35. Wagner S, Collet C, Madsen P, Nakashizuka T, Nyland RD, Sagheb-Talebi K. 2010 Beech regeneration research: From ecological to silvicultural aspects. *For. Ecol. Manage.* **259**, 2172–2182.

36. Hiraoka K, Tomaru N. 2009 Genetic divergence in nuclear genomes between populations of *Fagus crenata* along the Japan Sea and Pacific sides of Japan. *J. Plant Res.* **122**, 269–282.

37. Tateishi M, Kumagai T, Suyama Y, Hiura T. 2010 Differences in transpiration characteristics of Japanese beech trees, *Fagus crenata*, in Japan. *Tree Physiol.* **30**, 748–760.

38. Shimano K. 2002 Regeneration dynamics, causal factors, and characteristics of pacific ocean-type beech (*Fagus crenata*) forests in Japan: a review. *Folia Geobot.* **37**, 275–296.

39. Ichihara Y, Yamaji K. 2009 Effect of light conditions on the resistance of current-year *Fagus crenata* seedlings against fungal pathogens causing damping-off in a natural beech forest: fungus isolation and histological and chemical resistance. *J. Chem. Ecol.* **35**, 1077–1085.

40. Sahashi N, Kubono T, Shoji T. 1994 Temporal occurrence of dead seedlings of Japanese beech and associated Fungi. *J. Japanese For. Soc.* **76**, 338–345.

41. Yamaji K, Ichihara Y. 2012 The role of catechin and epicatechin in chemical defense against damping-off fungi of current-year *Fagus crenata* seedlings in natural forest. *For. Pathol.* **42**, 1–7.

42. Ono K, Yasuda Y, Matsuo T, Hoshino D, Chiba Y, Mori S. 2013 Estimating forest biomass using allometric model in a cool-temperate *Fagus crenata* forest in the Appi Highlands , Iwate , Japan. *Bull. For. For. Prod. Res. Inst.* **12**, 125–141.

43. Ishii HR, Horikawa S, Noguchi Y, Azuma W. 2018 Variation of intra-crown leaf plasticity of *Fagus crenata* across its geographical range in Japan. *For. Ecol. Manage.* **429**, 437–448.

44. Yamazaki JY, Yoda E, Takahashi A, Sonoike K, Maruta E. 2007 Pacific Ocean and Japan Sea ecotypes of Japanese beech (*Fagus crenata*) differ in photosystem responses to continuous high light. *Tree Physiol.* **27**, 961–968.

45. Okaura T, Harada K. 2002 Phylogeographical structure revealed by chloroplast DNA variation in Japanese Beech (*Fagus crenata* Blume). *Heredity.* **88**, 322–329.

46. Hasibeder R, Fuchslueger L, Richter A, Bahn M. 2015 Summer drought alters carbon allocation to roots and root respiration in mountain grassland. *New Phytol.* **205**, 1117–1127.

47. Mori S, Hagihara A. 1988 Respiration in stems of hinoki (*Chamaecyparis obtusa*) trees. *J. Japanese For. Soc.* **70**, 481–481.

48. Root respiration in *Chamaecyparis obtusa* trees. *Tree Physiol*. **8**, 217–225.

49. Niklas KJ, Hammond ST. 2014 Assessing Scaling Relationships: Uses, Abuses, and Alternatives. *Int. J. Plant Sci.* **175**, 754–763.

50. Hammer Ø, Harper DAT, Ryan PD. 2001 Past: Paleontological statistics software package for education and data analysis. *Palaeontol. Electron.* **4**, 1–9.

51. Lloret F, Casanovas C, Peñuelas J. 1999 Seedling survival of Mediterranean shrubland species in relation to root:shoot ratio, seed size and water and nitrogen use. *Funct. Ecol.* **13**, 210–216.

52. Padilla FM, Miranda JDD, Pugnaire FI. 2007 Early root growth plasticity in seedlings of three Mediterranean woody species. *Plant Soil* **296**, 103–113.

53. Paz H. 2003 Root/shoot allocation and root architecture in seedlings: variation among forest sites, microhabitats, and ecological groups. *Biotropica* **35**, 318–332.

54. Kitajima K. 1994 Relative importance of photosynthetic traits and allocation patterns as correlates of seedling shade tolerance of 13 tropical trees. *Oecologia* **98**, 419–428.

55. Cavender-Bares J, Bazzaz FA. 2000 Changes in drought response strategies with ontogeny in *Quercus rubra*: implications for scaling from seedlings to mature trees. *Oecologia* **124**, 8–18.

56. Ishida A, Yazaki K, Hoe AL. 2005 Ontogenetic transition of leaf physiology and anatomy from seedlings to mature trees of a rain forest pioneer tree, *Macaranga gigantea*. *Tree Physiol.* **25**, 513–522.

57. Thomas SC. 2010 Photosynthetic capacity peaks at intermediate size in temperate deciduous trees. *Tree Physiol.* **30**, 555–573.

58. Atkin O. 2010 Recommendation of [Mori S et al. at *Proc. Natl. Acad. Sci. USA*. 2010, **107**, 1447–1451]. In F1000Prime

59. Ballesteros FJ, Luque B. 2018 Gravity and life. In *Habitability of the universe before earth* (eds R Gordon & A Sharov), Vol. 1, pp. 3–26. Academic Press, Cambridge

60. Enquist BJ, Bentley LP. 2012 Land plants: New theoretical directions and empirical prospects. In R. M. Sibly, J. H. Brown, & A. Kodric-Brown (Eds.), *Metabolic ecology: A scaling approach* (pp. 164–187). Chichester: Wiley-Blackwell.

61. Kenrick P, Crane PR. 1997 The origin and early evolution of plants on land. *Nature* **389**, 33–39.

62. Raven JA, Edwards D. 2017 Roots: evolutionary origins and biogeochemical significance. *J. Exp. Bot.* **52**, 381–401.

63. Eissenstat DM, Wells CE, Yanai RD, Whitebeck JL. 2009 Building roots in a changing environment: implications for root longevity. *New Phytol.* **147**, 33–42.

64. Weemstra M, Mohren GMJ, Sterck FJ, Mommer L, van Ruijven J, Visser EJW, Kuyper TW. 2016 Towards a multidimensional root trait framework: a tree root review. *New Phytol.* **211**, 1159–1169.

65. McCormack ML *et al.* 2017 Building a better foundation: improving root-trait measurements to understand and model plant and ecosystem processes. *New Phytol.* **215**, 27–37.

66. Reich PB, Tjoelker MG, Machado JL, Oleksyn J. 2006 Universal scaling of respiratory metabolism, size and nitrogen in plants. *Nature* **439**, 457–461.

Chapter 2

Scaling of fresh mass, surface area, and root and shoot respiration of *Fagus crenata* from seeds to mature trees

Studies of terrestrial plant ecology and evolution have focused on the patterns of metabolic product allocation to roots and shoots in individual plants and the scaling of whole-plant respiration. However, few empirical studies have investigated the root:shoot ratio by considering the scaling of whole-plant respiration at various sizes throughout ontogeny. Here, using 377 individuals of *Fagus crenata* from five different Japanese provenances, we measured the respiration rates, surface area, and fresh mass of the entire roots and shoots, from germinating seeds to mature trees. We found that the relatively stable allometry of whole-plant respiration from seedlings to mature trees resulted from the integration of a convex upward curve of the root and a convex downward curve of the shoot to whole-plant fresh mass on the log-log coordinates. This suggests a gradual ontogenetic shift in allocation priority, from water uptake in seedlings to carbon gain in mature trees. We propose that this size-related root and shoot shift is common in *F. crenata*, regardless of the environment or phylogeny. Rapid root growth in early growth stage may promote subsequent shoot growth, and approaching the saturation of root growth may cause a decline in shoot and whole-plant growth during the mature stage.

1. Introduction

Comparative studies of terrestrial plant ecology and evolution focus on elucidating the variation of root:shoot mass ratio because of the allocation of metabolic production [1]. The allocation of metabolic production in plants is a zero-sum dynamic due to a trade-off between organs with contrasting roles [2]. Allocation to the structure and function of shoots may enhance carbon gain but must be at the expense of water uptake by roots, and vice versa. The optimal partitioning theory suggests that plants should allocate biomass to organs that require the most restricted resources in variable environments [1,3]. Many studies have supported this theory; however, the allocation is also likely to be regulated by differences in plant size [4–7]. The relationships between biomass allocation and plant size have often been studied using allometric analyses. Several studies have suggested that there are general allometric scaling rules for terrestrial plants that constrain allocation according to plant size [2,8]. Other studies suggest a continuous shift in the scaling exponent of such allometric relationships along plant size [6]. Nevertheless, few empirical studies are comparing the metabolic rate or resource acquisition area between roots and shoots at the whole-plant level in a wide range of plant sizes, including trees. Hence, uncertainty regarding the allocation of metabolic production with body size remains, and how the combined effects of variation in body size and environmental conditions alter the root:shoot ratio is not fully understood.

Respiration provides energy for the growth of organisms and elucidating the relationships between whole-plant respiration and plant size is crucial for the terrestrial plant growth model [9,10]. It is widely accepted that metabolic rates scale with body mass to the 3/4-power across various organisms. This is known as Kleiber's law [11], and theoretically explained by WBE model [12]. However, the universality of the metabolic scaling remains unclear [12–14]. To solve this question with empirical data, we have previously investigated the scaling of whole-plant

respiration by measuring 271 excavated trees including roots across nine orders of magnitude in mass up to 10^4 kg, including various tree species from Siberian to Southeast Asian biomes [15]. We found that the scaling of whole-plant respiration indicated a shift in the scaling exponent (i.e., a slope on the log-log coordinates) from 1.0 to 0.75 in the transition from seedlings to mature trees. This finding has implications for physiochemical constraints on the metabolic scaling of terrestrial plants [15–19]. The metabolic theory of ecology predicts that plant productivity and biomass are both size-dependent, and thus the physiochemical constraints will ultimately impact the dynamics of these factors [9]. However, the relationship between plant size throughout ontogeny and respiration changes in the entire root system remains unclear.

One of the goals of biological studies is to understand the general principles governing plant form and function of various species, with a particular focus at the individual level [11,12]. Elucidating the scaling of such individual-level physiology is a challenge for understanding the relationships between individual organisms and the emergent properties of ecosystems, such as productivity and resilience [20–22]. In plant ecology, integrating shoots and roots into whole-plant forms and functions have recently become increasingly important [23]. The individual-level form and function reflect adaptive processes that have been shaped over evolutionary timescales [20]. Given that the evolution of terrestrial plants has been accompanied by root development [24], comparing root and shoot respiratory scaling among species will assist in understanding the principles of plant form and function from an evolutionary perspective.

In another study, using *F. crenata* seedlings from the current year and those that were up to 1 year old, we found that in the root fraction (root/whole plant, %), size-dependent increases in respiration, fresh mass, and surface were likely to be specific to the early growth stage [19]. Considering the high mortality rate of *F. crenata* in the early growth stage, preferential root growth may be an important process to enhance water uptake and help avoid seedling death. It is

expected that the rapid root growth helps to increase photosynthetic performance by enhancing the water and nutrient uptake, and the preferential allocation would shift to shoot growth after the early growth stage [19]. The present study on *F. crenata* is the first step towards exploring the principle of form and function of terrestrial plants, by testing the scaling of roots and shoots in terms of respiration and surface area. Whole-plant respiration has been usually estimated by measuring portions within individuals [25–27]. We aimed to study the scaling of whole-plant respiration by investigating the respiration of entire shoots and roots over a wide range of plant sizes, considering the successive processes for water uptake and carbon acquisition during the course of ontogeny. In this study, we consistently used whole-plant closed chambers and conducted each respiration measurement per individual tree to establish a reliable dataset that encompasses the course of ontogeny.

The purpose of this study was to understand the scaling of whole-plant respiration and surface area, integrating the roots and shoots of *F. crenata*. *Fagus crenata* is widely distributed in Japan and often dominates typical cool-temperate deciduous forests [28]. The climatic conditions of the coastal areas in the Japan Sea and the Pacific Sea are characterised by heavy and light snowfall, respectively. Fujii et al. (2002) [28] analysed chloroplast DNA haplotypes across the distribution range of *F. crenata* and reported that the clades of this species are largely divided between the Japan Sea and Pacific Ocean sides of the Japanese Archipelago. Variations among the provenances or regions of *F. crenata* have also been reported to alter the morphological and physiological properties of the shoots, such as the transpiration rate, leaf area, and leaf thickness [29,30]. This study shows that the shoot–root balance changes dynamically during ontogeny depending on size by using trees from various provenances and environments. We suggest that the scaling of whole-plant respiration is generated from a size-dependent shift in the shoot–root balance. The findings from our empirical and novel approach will provide a basis to understand

the mechanisms of tree growth based on whole-plant physiology and to evaluate the impact of environmental changes on population dynamics.

2. Materials and Methods

(a) Plant materials and datasets

We used 377 *F. crenata* individuals in a wide range of sizes, with their developmental stage ranging from germinating seeds to mature trees of approximately 80 years of age. The plants were produced in five provenances in Japan that have different climatic conditions (see figure 2.1 for the geographical distribution of the five provenances of the plants used in our measurements and table 2.1 for the number of materials by the provenances).

To understand the scaling of whole-plant respiration with consideration of the balance between carbon acquisition and water uptake via true leaves and roots, we categorised plants into "germinating seeds–cotyledon stage" and "seedlings (with true leaves)–mature stage" groups. The "germinating seeds–cotyledon stage" refers to the period when the seed has absorbed water and germinated— expanding the cotyledons but before the development of the first true leaves— during which individual growth depends on the seed reserves in the cotyledons. For the seedlings to mature stage, we separated individuals into shoot and root and measured their respiration rate, fresh mass, and surface area. For the germinating seeds to the cotyledon stage, we only measured whole-plant respiration and fresh mass using intact individuals.

The plants of the "germinating seeds–cotyledon stage" group were prepared by sowing the seeds collected in Yamagata. For the plants of seedlings–mature stage, to cover the possible plasticity of respiration rates at various plant sizes, sampling was conducted in a variety of growth environments, across large gradients of tree density and light availability. Therefore, both suppressed (in more light-limited conditions) and dominant (in sufficient light conditions)

individuals were included in our measurements. The dataset included data reported in our previous studies [15,19] and the data obtained during this work.

.

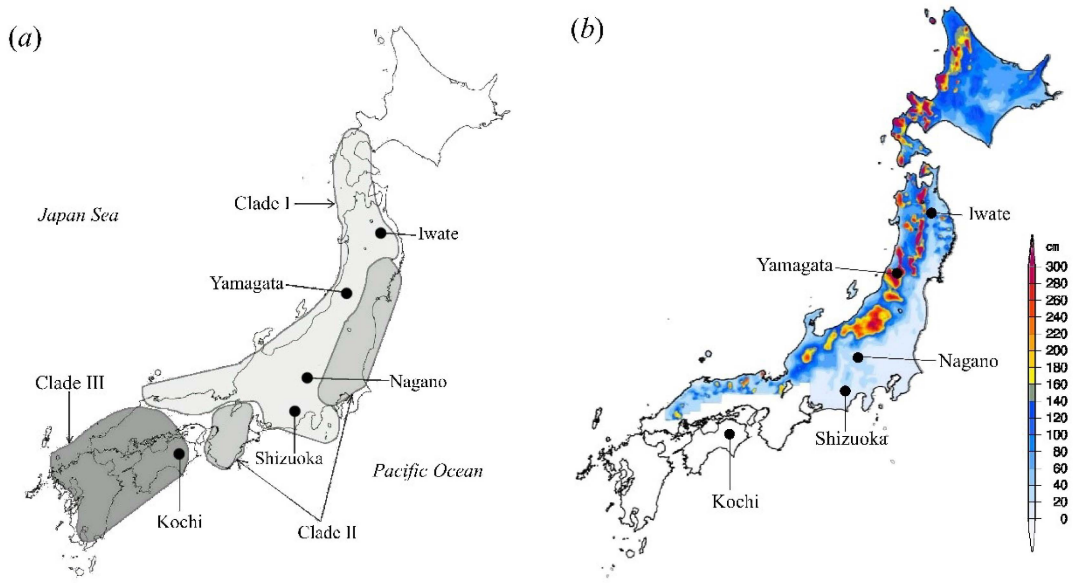

Figure 2.1 The five provenances where the individuals of *Fagus crenata* we used for our measurements were located, with (*a*) depicting three clades of *F. crenata* based on the chloroplast DNA analysis and (*b*) showing geographical variation in annual maximum snow depths in Japan. Two major clades (I and II+III) have been revealed in phylogenetic analyses among the haplotypes of *F. crenata*. Figure (*a*) is redrawn from Fujii et al. (2002). The data of annual maximum snow depth in figure (*b*) is from the Japan Meteorological Agency.

Table 2.1 Sample size (*n*) per provenance for the measurement of respiration, fresh mass, and surface area

Growth stage	Provenance	Whole-plant fresh mass	Shoot fresh mass	Root fresh mass	Whole-plant respiration	Shoot respiration	Root respiration	Whole-plant surface area	Shoot surface area	Root surface area
Germinating seeds–cotyledon stage	Yamagata	39	0	0	39	0	0	0	0	0
Seedlings–mature stage	Yamagata	236	236	236	166	166	166	140	141	147
	Iwate	58	59	58	58	59	58	0	0	0
	Kochi	14	14	14	14	14	14	9	9	12
	Shizuoka	8	8	8	8	8	8	5	7	5
	Nagano	21	21	21	21	21	21	0	0	0
Total		376	338	337	306	268	267	154	157	164

(b) Measurement of respiration rate, surface area, and fresh mass

Respiration rates of the plants in the developmental stages of germinating seeds to mature trees were measured at the whole-plant level per individual using the methods developed by Mori et al. (2010) [15] (figure 2.2). After being excavated, individuals of germinating seeds–cotyledonary stage were left intact and the seedling–adult trees were cut into shoot and root. After the measurement of the fresh mass, we covered them with a wet cloth to prevent transpiration and measured their respiration rates [15,31]. The measurement of respiration was completed within 20 min after the excavation. The plant materials were enclosed in customised incubation chambers, and the CO_2 concentration within the chamber was measured every 5 s for approximately 30–300 s with a CO_2 probe (GMP343, Vaisala, Helsinki, Finland). During the measurements, the CO_2 concentration in the chamber was homogenised using forced air circulation with DC axial fans. In large volume chambers, a cylindrical air duct attached to the fans facilitated sufficient air circulation. To obtain accurate measurements in a short time, a chamber that is too large for the materials should not be used. Therefore, suitable chamber sizes were selected from 10 chambers of various volumes (80 cm^3 to 8 m^3) according to the size of the shoots and roots. To avoid temperature variation influencing respiration rates [32], all the calculated respiration rates were adjusted to 20 °C, assuming $Q_{10} = 2$.

The measurement of whole-plant surface area was performed for the plants of seedlings–mature stage. The shoot surface area was calculated as the sum of the leaf and surface areas of the stems and branches. The leaf area was measured using a leaf area metre (LI-3100C; LICOR, Lincoln, NE, USA). The surface areas of the stems and branches were calculated from their diameter and length, assuming that they were cylindrical [25,33]. The root surface area was evaluated using the image analysis software WinRhizo version 2016a (Regent Instruments, Quebec, Canada) in cases where the root diameter was less than 2 cm. The root images for analysis

were obtained using a flatbed scanner (Epson Perfection V800, Seiko Epson, Japan) at a resolution of 800 dpi. When the root diameter exceeded 2 cm, the root surface area was calculated from their diameter and length, assuming that they were cylindrical.

Figure 2.2 Measurement of whole-plant respiration using closed-air circulation chamber. (*a*) measurement of excavated whole root from a mature tree. (*b*) Sealing of the material from a mature tree in the chamber. (*c*) The roots of a mature tree immediately after excavation. (*d*) Measurement of the germinating seeds, using the smallest chamber (80 cm^3). The seeds are wrapped in a wet sheet and attached to the top cover of the chamber. A small fan is attached to the inside of the sensor head.

(c) Data analysis

The relationships between respiration rate (μmol CO_2 s^{-1}), fresh mass (kg), and surface area (m^2) were plotted on the log-log coordinates, and two types of trends were observed: linear trend, and curve trend (convex upward or convex downward) that gradually change the scaling exponent. Using these trends as candidates, we selected a model for each scaling relationship. The linear model on log-log coordinates is expressed as a simple power function as

$$Y = FM^f, \quad (2)$$

where M is the explanatory variable (e.g., fresh mass or surface area), Y is the response variable (e.g., respiration rate), F is the intercept, and f is the scaling exponent (slope on the log-log coordinates). The convex trends on the log-log coordinates are expressed as follows [34]:

$$\frac{1}{Y} = \frac{1}{GM^g} + \frac{1}{HM^h} \ (g > h) \quad (2)$$

or

$$Y = GM^g + HM^h \ (g > h), \quad (3)$$

where G and H are the coefficients, and g and h are the exponents. As M varies, they approach the following asymptotic relationships:

$$Y = GM^g \quad (4)$$

$$Y = HM^h. \quad (5)$$

When $GM^g \ll HM^h$, Eq. 2 approaches Eq. 4, and Eq. 3 approaches Eq. 5. When $GM^g \gg HM^h$, Eq. 2 approaches Eq. 5, and Eq. 3 approaches Eq. 4. These mixed-power functions are flexible enough to capture continuous ontogenetic shifts in the scaling exponents with plant size [15]. When point P on the log-log coordinates denotes the intersection between the two asymptotic lines, or Eqs. 4 and 5, the value of M at point P is calculated as $(H/G)^{[1/(g-h)]}$. At $M = (H/G)^{[1/(g-h)]}$, the slope of the line that is tangent to Eqs. 2 and 3 is $(g+h)/2$ [15].

The regression analysis was performed using the Levenberg-Marquardt algorithm (LMA) [35] using the nlsLM function in minpack.lm from the R package [36]. We compared the three models using Akaike's Information Criterion (AIC) and deemed the model with the lowest AIC as the best fit [37]. Using the Bayesian Information Criterion (BIC) did not change our results. In the case where the linear model was the best, we conducted a reduced major axis (RMA) regression analysis [38] of the log-transformed version of Eq. 1 using the PAST analysis software [39]. Finally, using the obtained functions for the relationships of root and shoot to whole-plant fresh mass, we tested how with respect to respiration, fresh mass, and surface area, the root fraction (roots/total plant, %) shifted in the seedlings–mature stage.

3. Results

(a) Germinating seeds to mature trees (scaling of whole-plant respiration)

In our dataset, whole-plant fresh mass for germinating seeds–cotyledon stage ranged between 0.0000954 kg and 0.000470 kg (n = 39), and for seedlings–mature stage, between 0.000276 kg and 583 kg (n = 267). To consider the scaling of whole-plant respiration in the ontogeny from seed germination to mature trees, the data sets for these two growth stages were combined and analysed. The relationship between whole-plant respiration and whole-plant fresh mass showed a convex upward trend on the log-log coordinates in Eq. 2 (n = 306, figure 2.3*a*, see table 2.2 for the AIC). With increasing plant mass, the exponent decreased from 3.49 to 0.763. The whole-plant fresh mass at the asymptotes' intersection point P was 0.000263 kg. These observations indicated that the scaling exponent was considerably high, exceeding 3.0 in the period from seed germination to before true leaves develop, and decreased gradually to 0.75 in mature trees.

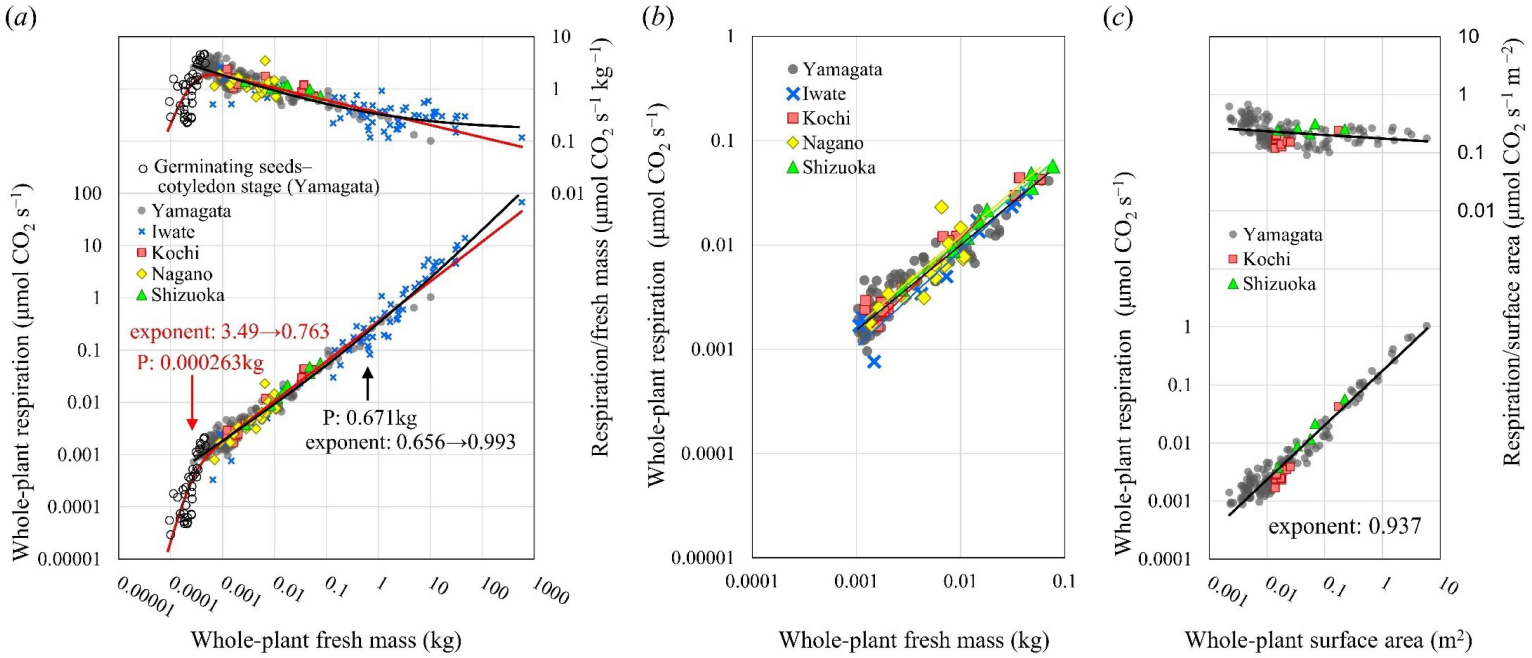

Figure 2.3 Scaling of whole-plant respiration versus whole-plant fresh mass (*a*), comparison of whole-plant respiration among provenances (*b*), and the scaling of whole-plant respiration versus whole-plant surface area (*c*). The solid lines in figures *a* and *c* indicate the best fit model for each relationship (red line: germinating seeds to mature stage, black line: seedlings to mature stage). In figure *a*, changes in the scaling exponent with increasing plant size are shown. The point P represents the whole-plant fresh mass at the asymptotes' intersection of the curve trends. No significant differences were observed among provenances in the results of reduced major axis regression analysis in figure *b*. The dataset of germinating seeds–cotyledon stage in figure *a* is not included in figures *b*, *c,* and figures 2.4–2.8.

Table 2.2 Results of fitting analysis and goodness of fit (AIC and BIC statistics) for the scaling of whole-plant respiration rates with whole-plant fresh mass and whole-plant surface area (figure 2.3*a*, *c*).

Growth stage in dataset	Relationship	Equation	Trend	AIC	BIC	*F*	*G*	*H*	*f*	*g*	*h*
Germinating seeds to mature stage	Whole-plant respiration vs. whole-plant fresh mass (figure 2.3*a*, $n = 306$)	Eq. 1		554.77	565.95	0.3913 (2.477×10^{-2})			0.8133 (1.068×10^{-2})		
		Eq. 2	**Convex upward**	**433.08**	**451.70**		**2.066×10^{9}** (6.177×10^{9})	**0.353** (1.856×10^{-2})		**3.491** (0.3465)	**0.7626** (1.049×10^{-2})
		Eq. 3		479.67	498.29		0.3656 (1.319×10^{-2})	-6.881×10^{-4} (2.051×10^{-2})		0.757 (0.1903)	8.734×10^{-2} (1.957×10^{-2})
Seedlings to mature stage	Whole-plant respiration vs. whole-plant fresh mass (figure 2.3*a*, $n = 267$)	Eq. 1		255.56	266.32	0.3546 (1.479×10^{-2})			0.7688 (7.606×10^{-3})		
		Eq. 2		259.56	277.49		0.3547 (71.86)	2037 (2.371×10^{9})		0.7688 (8.592)	0.7685 (4.945×10^{4})
		Eq. 3	**Convex downward**	**237.29**	**255.23**		**0.1756 (0.1027)**	**0.1538 (9.318×10^{-2})**		**0.9929 (0.1145)**	**0.6558 (6.782×10^{-2})**
	Whole-plant respiration vs. whole-plant surface area (figure 2.3*c*, $n = 152$)	**Eq. 1**	**Linear**	**145.95**	**155.02**	**0.1566 (1.212×10^{-2})**			**0.909 (0.01872)**		
		Eq. 2		149.95	165.07		7.916 (1.078×10^{7})	0.1598 (4390)		0.9087 (8226)	0.9086 (166.1)
		Eq. 3		149.95	165.07		0.2257 (9.828×10^{4})	-6.903×10^{-2} (9.828×10^{4})		0.90864 (737.0)	0.90863 (2408)

Equation 1: $\ln Y = \ln F + f \ln M$. Equation 2: $\ln Y = -\ln [1/(GM^{g}) + 1/(HM^{h})]$. Equation 3: $\ln Y = \ln (GM^{g} + HM^{h})$. Fitting analysis was performed using the nlsLM. The numbers in parentheses indicate the standard error of the mean for each parameter. The model with the lowest AIC value is highlighted in bold.

(b) Seedlings to mature trees

(i) Scaling of whole-plant respiration

For the dataset of seedlings–mature stage ($n = 267$), the relationship between whole-plant respiration and whole-plant fresh mass on the log-log coordinates was best fitted by Eq. 3, describing a convex downward trend (figure 2.3*a*, see table 2.2 for the AIC). With increasing plant mass, the exponent increased from 0.656 to 0.993. The whole-plant fresh mass at the intersection point P was 0.671 kg. All the data were plotted close to a single line, suggesting that respiration of individual plants from different provenances and environments is, to some extent, equally controlled by size. A linear fit was also determined. In OLS, the scaling exponent was 0.769 (95% confidence interval (CI): 0.751–0.789) and the intercept was 0.355 (95% CI: 0.320–0.399). In RMA, the exponent was 0.779 (95% CI: 0.762–0.797) and the intercept was 0.371 (95% CI: 0.337–0.413). These were obtained with a sufficient coefficient determinant value, $R^2 = 0.975$. Therefore, considering the ontogeny from seedlings to mature trees, scaling of whole-plant respiration to whole-plant fresh mass in our results was well expressed by a linear trend, with the scaling exponent slightly larger than, but close to, 0.75, as proposed by Kleiber's law [11] and WBE model [12].

Within 0.001 kg–0.1 kg of the whole-plant fresh mass, scaling of the whole-plant respiration of the *F. crenata* individuals from the five provenances were compared by RMA regression analysis (Eq. 1). For all the five provenances, the 95% CI of the scaling exponent included 0.75. There was an overlap between the 95% CI of scaling exponents and the intercepts among all provenances (figure 2.3*b*, table 2.3), suggesting that there were no significant differences in the size-response of seedling whole-plant respiration among the provenances.

For the relationships between whole-plant respiration and whole-plant surface area, the best model was the linear trend of Eq. 1 (figure 2.3*c*, see table 2.2 for AIC). Whole-plant surface area ranged between 0.00225 m^2 and 5.89 m^2 ($n = 152$). Whole-plant surface area ranged between 0.00225 m^2 and 5.89 m^2 ($n = 152$). RMA regression analysis had the scaling exponent of 0.937 (95% CI: 0.908–0.971) and the intercept of 0.174 (95% CI: 0.157–0.200) in $R^2 = 0.940$, suggesting consistently negative allometry (exponent < 1.0).

Table 2.3 Results of reduced major axis (RMA) regression (Equation 1: ln Y = ln F+f ln M) showing the relationships between whole-plant respiration and whole-plant fresh mass for each provenance using the data of plants within the weight range of 0.001 kg–0.1 kg (figure 2.3*b*).

Provenance	*n*	Range of whole-plant fresh mass (kg)	Slope	95%CI of Slope	Intercept	95%CI of Intercept	R^2
Iwate	10	0.00106–0.0428	0.927	0.705–1.08	0.632	0.254–1.21	0.930
Kochi	14	0.00121–0.058	0.866	0.722–0.953	0.652	0.295–1.00	0.959
Nagano	19	0.00141–0.0157	1.00	0.662–1.24	1.16	0.177–4.40	0.713
Shizuoka	8	0.00273–0.0767	0.843	0.750–0.926	0.540	0.350–0.741	0.983
Yamagata	96	0.00103–0.07	0.816	0.754–0.865	0.427	0.292–0.571	0.873

(ii) Scaling of surface area in the whole plant, shoots, and roots

The log-log plots of the relationships between the surface area and fresh mass in the whole plant, shoot, and root along with the selected best model are shown in figure 2.4*a*,*b* (see table 2.4 for AIC).

Considering the scaling of the whole-plant surface area, Eq. 2 had the best fit with a convex upward trend. The whole-plant fresh mass ranged between 0.000413 kg and 10.2 kg (n = 154). The exponent shifted from 1.48 to 0.654 with an increasing whole-plant fresh mass, and the whole-plant fresh mass at the intersection point P was 0.000987 kg.

The scaling of the shoot surface area was best fitted by the linear trend of Eq. 1. Shoot fresh mass ranged between 0.000287 kg and 7.29 kg (n = 157). RMA regression analysis provided the scaling exponent of 0.806 (95% CI: 0.783–0.829) and the intercept of 1.49 (95% CI: 1.27–1.74) in R^2 = 0.985, suggesting consistently negative allometric trends. The scaling of the root surface area was best fitted by Eq. 2, describing a convex upward trend. Root fresh mass ranged between 0.0000330 kg and 2.91 kg (n = 164). The scaling exponents decreased from 1.59 to 0.477 with increasing root fresh mass, and the root fresh mass at the point P was 0.00126 kg.

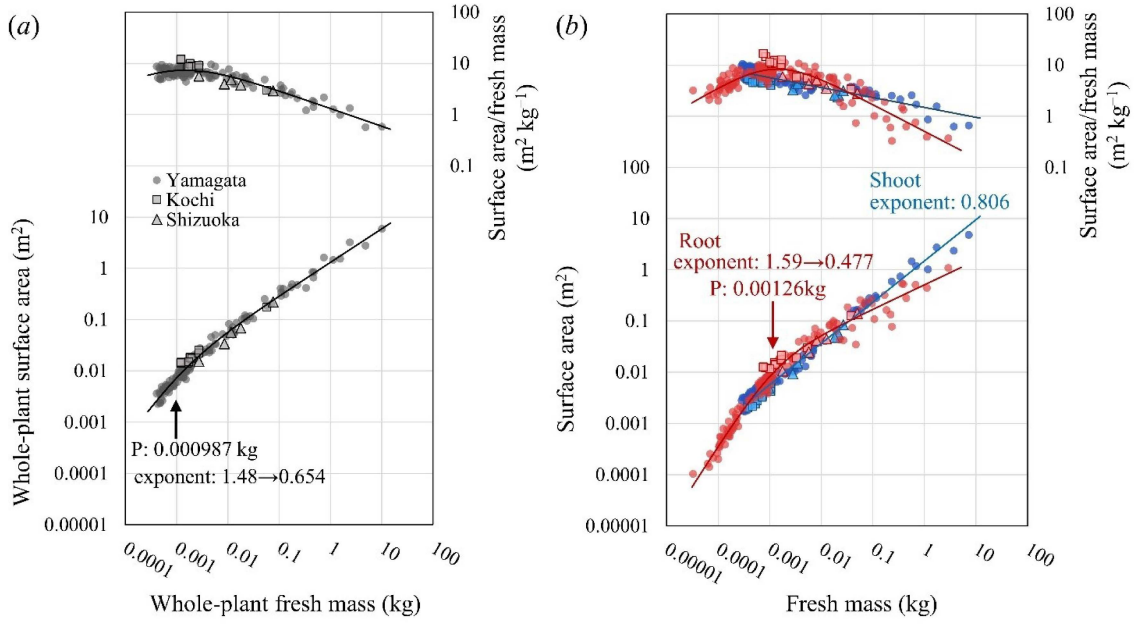

Figure 2.4 Scaling relationships between surface area and fresh mass in whole plant (*a*) and the relationships in the shoot (blue) and root (red) (*b*). For the relationships best fitted by curve trends, changes in the scaling exponent with increasing fresh mass are shown in figures. The point P represents the fresh mass at the asymptotes' intersection of the curve trends.

Table 2.4 Results of fitting analysis and goodness of fit (AIC and BIC statistics) for the scaling of surface area with fresh mass for the whole plant, shoot, and root using the dataset of the individuals of seedlings–mature stage (figure 2.4*a*, *b*).

Relationship	Equation	Trend	AIC	BIC	*F*	*G*	*H*	*f*	*g*	*h*
Whole-plant surface area vs. whole-plant fresh mass (figure 2.4*a*, *n* = 154)	Eq. 1		10.95	20.06	1.671 (9.300×10^{-2})			0.7806 (9.397×10^{-3})		
	Eq. 2	**Convex upward**	**−72.63**	**−57.44**		**393.1 (448.1)**	**1.314 (6.449×10^{-2})**		**1.477 (0.1439)**	**0.6536 (2.472×10^{-2})**
	Eq. 3		14.95	30.13		0.4004 (4.469×10^{5})	1.270 (4.469×10^{5})		0.780648 (2355)	0.780641 (742.4)
Shoot surface area vs. shoot fresh mass (figure 2.4*b*, *n* = 157)	**Eq. 1**	**Linear**	**−44.96**	**−35.79**	**1.432 (7.504×10^{-2})**			**0.8001 (7.882×10^{-3})**		
	Eq. 2		−42.865	−27.58		-2.728×10^{5} (4.584×10^{6})	1.478 (9.229×10^{-2})		2.041 (2.019)	0.8116 (1.793×10^{-2})
	Eq. 3		−40.96	−25.68		1.306 (8.998×10^{4})	0.1264 (8.998×10^{4})		0.80016 (1891)	0.80014 (1.953×10^{4})
Root surface area vs. root fresh mass (figure 2.4*b*, *n* = 164)	Eq. 1		304.33	313.63	1.760 (0.250)			0.834 (2.103×10^{-2})		
	Eq. 2	**Convex upward**	**98.41**	**113.91**		**856.0 (511.9)**	**0.5075 (5.683×10^{-2})**		**1.591 (6.782×10^{-2})**	**0.4773 (3.428×10^{-2})**
	Eq. 3		308.33	323.83		0.1878 (5.027×10^{5})	1.571 (5.027×10^{5})		0.8343749 (1.524×10^{5})	0.8344745 (1.822×10^{4})

Equation 1: $\ln Y = \ln F + f \ln M$. Equation 2: $\ln Y = -\ln [1/(GM^{g}) + 1/(HM^{h})]$. Equation 3: $\ln Y = \ln (GM^{g} + HM^{h})$. Fitting analysis was performed using the nlsLM. The numbers in parentheses indicate the standard error of the mean for each parameter. The model with the lowest AIC value is highlighted in bold. (iii) Scaling of respiration with fresh mass and surface area for shoot and root

(iii) Scaling of respiration with fresh mass and surface area in shoot and root

For the shoot and root, log-log plots of the relationships between the respiration and fresh mass, and the respiration and surface, are shown in figures 2.5*a* and 2.5*b*, respectively, with the model with the lowest AIC (see table 2.5 for AIC).

The relationship between shoot respiration and shoot fresh mass was best fitted by the linear trend of Eq. 1. Shoot fresh mass ranged between 0.000210 kg and 521 kg (n = 268). RMA provided the exponent of 0.785 (95% CI: 0.768–0.805) and intercept of 0.403 (95% CI: 0.355–0.459) in R^2 = 0.968. The relationship between root respiration and root fresh mass was best fitted Eq. 3, describing a convex downward trend. Root fresh mass ranged between 0.000033 kg and 62.1 kg (n = 267). With increasing root fresh mass, the exponent increased from 0.672 to 1.25. Root fresh mass at P was 2.12 kg.

The relationship between shoot respiration and shoot surface area was best fitted by Eq. 2, describing a convex upward trend. Shoot surface area ranged between 0.0017 m^2 and 4.81 m^2 (n = 155), which corresponded to 0.000287 kg and 7.29 kg, respectively, of shoot fresh mass. The scaling exponents decreased from 1.38 to 0.753 with increasing shoot surface area. Shoot surface area at the intersection point P was 0.00970 m^2. The relationships between root respiration and root surface area were best fitted by Eq. 3, describing a convex downward trend. Root surface area ranged between 0.000103 m^2 and 1.08 m^2 (n = 162), which corresponded to 0.0000330 kg and 2.91 kg, respectively, of root fresh mass. The scaling exponent increased from 0. 414 to 1.32 with increasing root surface area. Root surface area at intersection point P was 0.0212 m^2.

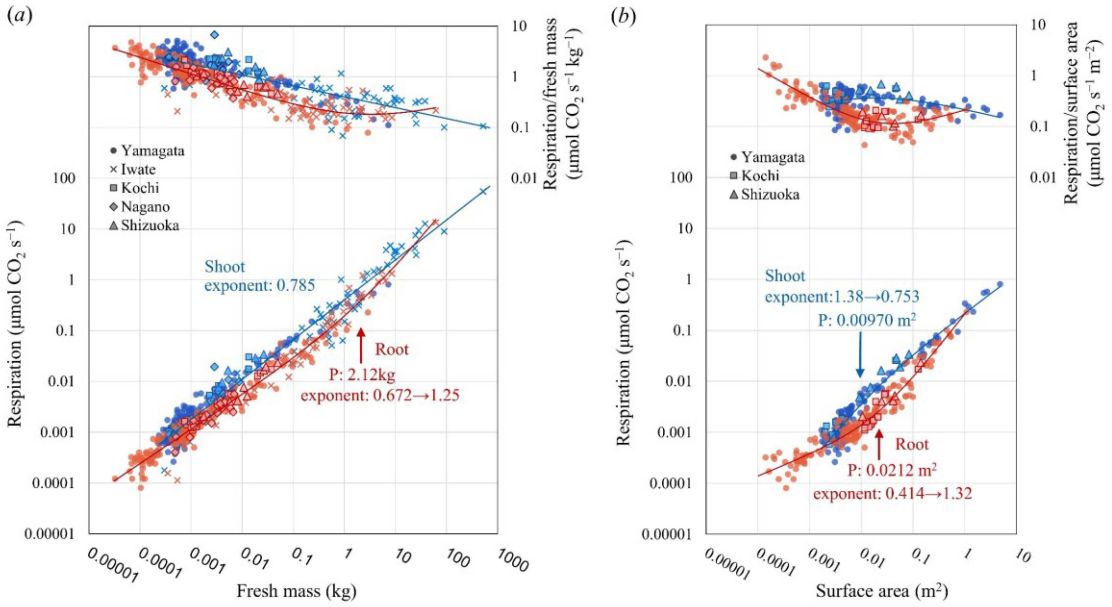

Figure 2.5 Scaling of the shoot and root respiration rates with fresh mass (*a*) and surface area (*b*). For the relationships best fitted by curve trends, changes in the scaling exponent with increasing fresh mass or surface area are shown in the figures. The point P represents the fresh mass or surface area at the asymptotes' intersection of the curve trends.

Table 2.5 Results of fitting analysis and goodness of fit (AIC and BIC statistics) for the scaling respiration rates in relation to fresh mass and surface area, for the shoot and root using the dataset of the individuals of seedlings–mature stage (figure 2.5*a*,*b*).

Relationship	Equation	Trend	AIC	BIC	*F*	*G*	*H*	*f*	*g*	*h*
Shoot respiration rate vs. shoot fresh mass (figure 2.5*a*, *n* = 268)	**Eq. 1**	**Linear**	**354.25**	**365.02**	**0.3778 (1.988×10^{-2})**			**0.7729 (8.574×10^{-3})**		
	Eq. 2		356.93	374.88		3651 (5.169×10^{4})	0.3757 (2.017×10^{-2})		1.677 (1.685)	0.7607 (2.069×10^{2})
	Eq. 3		357.02	374.98		0.376 (2.023×10^{-2})	-5.46×10^{-5} (8.201×10^{-4})		0.7617 (2.123×10^{-2})	-8.437×10^{-2} (1.753)
Root respiration rate vs. root fresh mass (figure 2.5*a*, *n* = 267)	Eq. 1		284.04	294.80	0.1841 (9.616×10^{-2})			0.7352 (8.487×10^{-3})		
	Eq. 2		288.04	305.98		0.5146 (5.242×10^{5})	0.2867 (1.627×10^{5})		0.73520 (355.3)	0.73519 (1.979×10^{3})
	Eq. 3	**Convex downward**	**254.02**	**271.95**		**0.0759 (2.861×10^{-2})**	**0.1175 (2.071×10^{-2})**		**1.253 (0.1437)**	**0.6723 (2.287×10^{-2})**
Shoot respiration rate vs. shoot surface area (figure 2.5*b*, *n* = 155)	Eq. 1		165.11	174.23	0.2553 (2.449×10^{-2})			0.9552 (1.931×10^{2})		
	Eq. 2	**Convex upward**	**158.24**	**173.46**		**4.114 (9.758)**	**0.2261 (3.808×10^{-2})**		**1.379 (0.3384)**	**0.7532 (0.1443)**
	Eq. 3		169.11	184.32		1.496×10^{-2} (2.329×10^{4})	0.2404 (2.329×10^{4})		0.9553 (1702)	0.9552 (105.2)
Root respiration rate vs. root surface area (figure 2.5*b*, *n* = 162)	Eq. 1		246.75	256.01	5.927×10^{-2} (6.218×10^{-3})			0.7509 (2.05×10^{-2})		
	Eq. 2		250.75	266.18		0.2984 (4.337×10^{5})	7.397×10^{-2} (2.665×10^{4})		0.7509 (1498)	0.7508 (371.5)

Eq. 3	**Convex downward**	**156.54**	**171.98**		**0.2044 (3.607×10^{-2})**	**6.248×10^{-3} (3.096×10^{-3})**	**1.319 (0.1094)**	**0.4144 (6.557×10^{-2})**

Equation 1: $\ln Y = \ln F + f \ln M$. Equation 2: $\ln Y = -\ln [1/(GM^g) + 1/(HM^h)]$. Equation 3: $\ln Y = \ln (GM^g + HM^h)$. Fitting analysis was performed using the nlsLM. The numbers in parentheses indicate the standard error of the mean for each parameter. The model with the lowest AIC value is highlighted in bold.

(iv) Scaling of the shoot and root respiration rates, fresh mass, and surface area in relation to whole-plant fresh mass

To analyse the ontogenetic shift in root-shoot balance from seedlings to mature trees, we conducted model selection for scaling of the shoot and root respiration, fresh mass, and surface area to whole-plant fresh mass. The log-log plots of shoot and root to whole-plant fresh mass are shown in figures 2.6*a–c* with fitting lines of the trend with the lowest AIC (see table 2.6 for AIC). We also conducted RMA regression analysis within 0.001 kg–0.1 kg and observed little difference in the scaling exponent among provenances (figure 2.7 and table 2.7).

The relationships of shoot respiration rate, fresh mass, and surface area to whole-plant fresh mass showed a convex downward trend in Eq. 3. In all cases, the scaling exponents for shoots shifted from smaller than 0 in small plants to larger than 0.8 in large plants; the exponent shifted from −0.918 to 0.864 for respiration (n = 267), from −0.0903 to 1.13 for fresh mass (n = 337), and from −0.218 to 0.946 for surface area (n = 157). The values of whole-plant fresh mass at point P were 0.000628 kg, 0.000888 kg, and 0.00135 kg for the shoot respiration rate, shoot fresh mass, and shoot surface area, respectively.

The relationships of root respiration rate, fresh mass, and surface area in relation to whole-plant fresh mass were convex upward in Eq. 2. In all cases, the scaling exponent shifted from larger than 2 in small plants to less than one in large plants; the exponent shifted from 2.35 to 0.638 for respiration (n = 267), from 2.50 to 0.825 for fresh mass (n = 337), and from 2.76 to 0.437 for surface area (n = 164). The values of whole-plant fresh mass at point P were 0.000558 kg, 0.00108 kg, and 0.00196 kg for the root respiration rate, root fresh mass, and root surface rea, respectively.

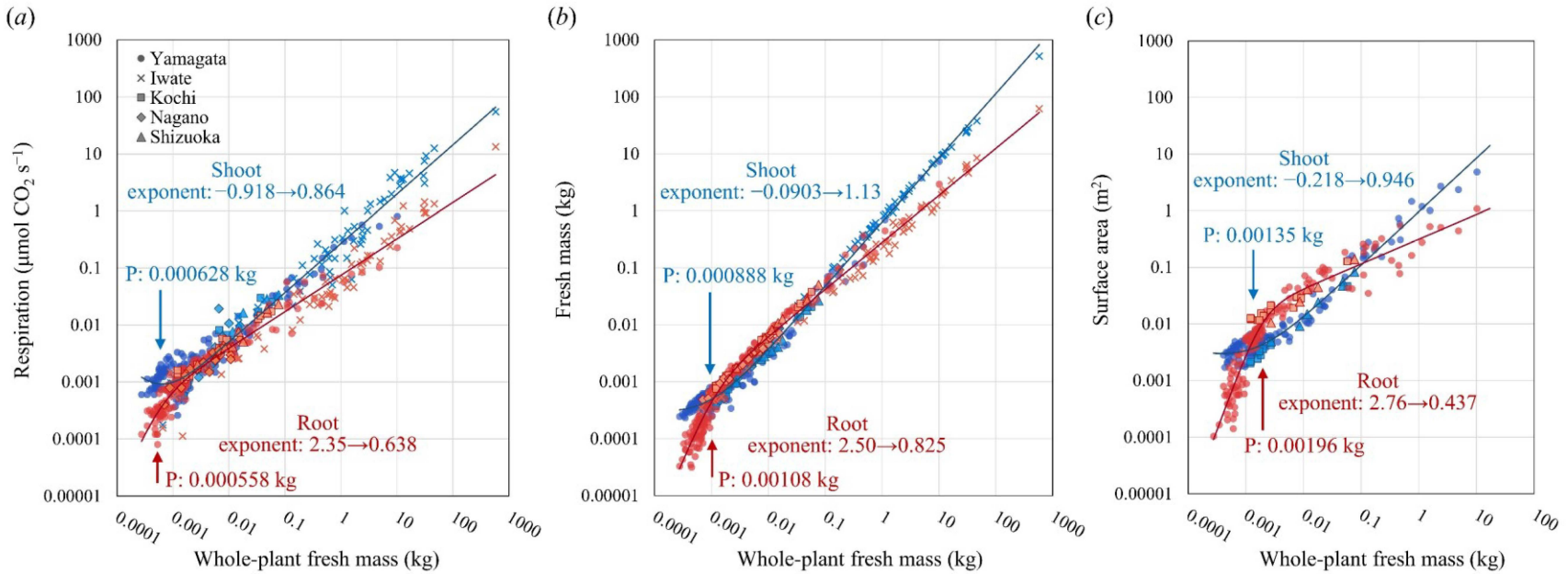

Figure 2.6 Relationships between shoot and root respiration rate (*a*), fresh mass (*b*), and surface area (*c*) in relation to whole-plant fresh mass. For each relationship, change in the scaling exponent with increasing whole-plant fresh mass is shown in the figures. The point P represents the whole-plant fresh mass at the asymptotes' intersection of the curve trends.

Table 2.6 Results of fitting analysis and goodness of fit (AIC and BIC statistics) for scaling of the shoot and root respiration, fresh mass, and surface area in relation to the whole-plant fresh mass using the dataset of individuals of seedlings–mature stage (figure 2.6*a–c*).

Dependent variable	Equation	Trend	AIC	BIC	*F*	*G*	*H*	*f*	*g*	*h*
Shoot respiration (figure 2.6*a*, $n = 267$)	Eq. 1		449.91	460.67	0.2556 (1.534×10^{-2})			0.8046 (1.094×10^{-2})		
	Eq. 2		453.91	471.85		53.42 (8.716×10^{7})	0.2569 (2015)		0.8048 (5567)	0.8046 (26.78)
	Eq. 3	**Convex downward**	**398.40**	**416.34**		**0.2697 (0.01476)**	**5.290×10^{-7} (1.590×10^{-6})**		**0.8641 (0.01617)**	**−0.9181 (0.3925)**
Root respiration (figure 2.6*a*, $n = 267$)	Eq. 1		373.17	383.93	7.801×10^{-2} (4.055×10^{-3})			0.6901 (9.479×10^{-3})		
	Eq. 2	**Convex upward**	**321.72**	**339.66**		**2.703×10^{4} (7.890×10^{4})**	**0.07451 (3.532×10^{-3})**		**2.347 (0.3810)**	**0.6384 (1.414×10^{-2})**
	Eq. 3		330.98	348.91		7.565×10^{-2} (3.662×10^{-3})	-8.730×10^{-5} (1.986×10^{-4})		0.6373 (1.917×10^{-2})	−0.1621 (0.2629)
Shoot fresh mass (figure 2.6*b*, $n = 337$)	Eq. 1		288.67	300.13	0.588 (2.325×10^{-2})			1.031 (6.842×10^{-3})		
	Eq. 2		292.67	311.77		449.6 (3.423×10^{8})	0.589 (587.8)		1.03094 (60170)	1.03090 (78.86)
	Eq. 3	**Convex downward**	**50.51**	**69.61**		**0.634 (1.784×10^{-2})**	**1.23×10^{-4} (1.061×10^{-4})**		**1.126 (1.016×10^{-2})**	**−0.0903 (0.113)**
Root fresh mass (figure 2.6*b*, $n = 337$)	Eq. 1		510.85	522.31	0.3141 (1.726×10^{-2})			0.9478 (9.513×10^{-2})		
	Eq. 2	**Convex upward**	**186.94**	**206.04**		**2.563×10^{4} (22480)**	**0.2782 (9.546×10^{-3})**		**2.499 (0.117)**	**0.8247 (1.062×10^{-2})**

	Eq. 3		514.85	533.95		8.530×10^{-4} (899.3)	0.3133 (899.3)		0.947796 (4.730×10^{5})	0.947795 (1288)
Shoot surface area (figure 2.6*c*, $n = 157$)	Eq. 1		163.54	172.71	0.6521 (5.82×10^{-2})			0.7739 (1.513×10^{2})		
	Eq. 2		167.54	182.82		352.3 (5.691×10^{8})	0.6532 (1956)		0.7739 (3.563×10^{4})	0.7738 (66.14)
	Eq. 3	**Convex downward**	**77.88**	**93.16**		**0.9561 (0.07685)**	**4.363×10^{-4} (5.732×10^{-4})**		**0.946 (3.035×10^{-2})**	**−0.2180 (0.1738)**
Root surface area (figure 2.6*c*, $n = 164$)	Eq. 1		448.02	457.32	0.8749 (0.1822)			0.8238 (3.478×10^{2})		
	Eq. 2	**Convex upward**	**257.54**	**273.03**		**6.137×10^{5} (7.179×10^{5})**	**0.3128 (4.193×10^{-2})**		**2.760 (0.1616)**	**0.4374 (3.744×10^{-2})**
	Eq. 3		452.02	467.52		0.5897 (1.088×10^{6})	0.2852 (1.088×10^{6})		0.823777 (1.240×10^{4})	0.823775 (2.564×10^{4})

Equation 1: $\ln Y = \ln F + f \ln M$. Equation 2: $\ln Y = -\ln [1/(GM^{g}) + 1/(HM^{h})]$. Equation 3: $\ln Y = \ln (GM^{g} + HM^{h})$. Fitting analysis was performed using the nlsLM. The numbers in parentheses indicate the standard error of the mean for each parameter. The model with the lowest AIC value is highlighted in bold.

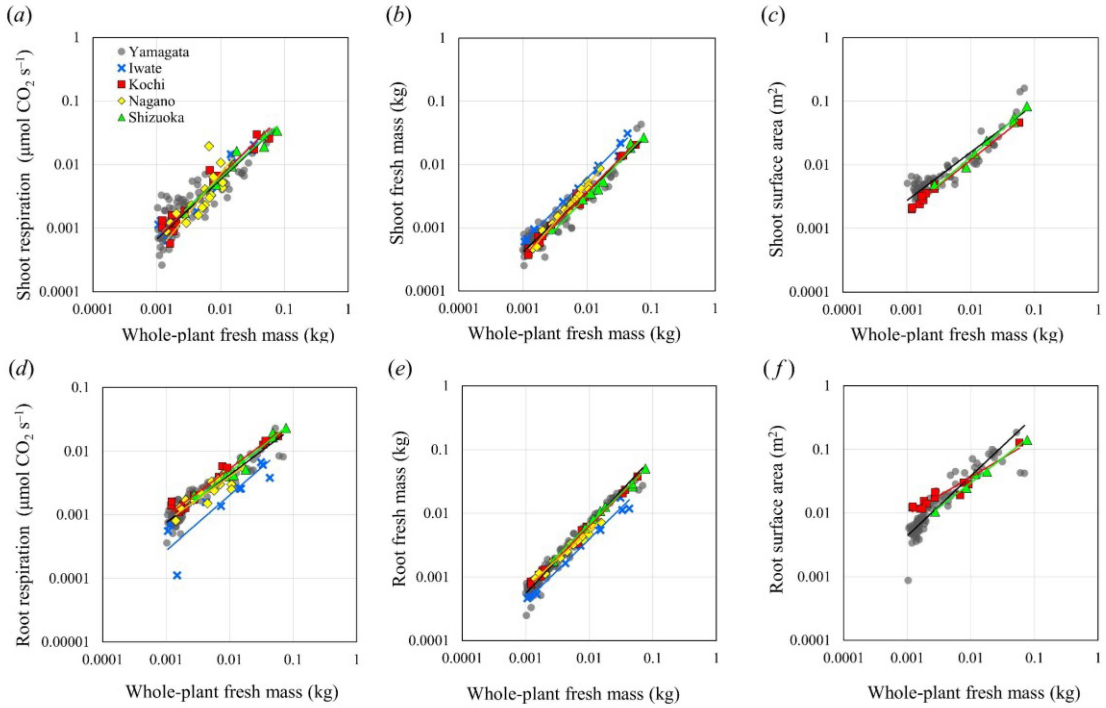

Figure 2.7 Comparison of the scaling relationships between respiration, fresh mass, and surface area of the shoot (*a*–*c*) and root (*d*–*f*) in relation to whole-plant fresh mass among provenances by reduced major axis (RMA) regression analysis. Root fresh mass and root respiration of Iwate plants appear to be lower than those of other provenances. This may be due to the higher water availability and more limited light availability in the environment where the Iwate plants were collected, compared to those of other provenances. Nevertheless, the RMA regression analysis did not show noticeable differences among provenances as shown in table 2.7.

Table 2.7 Results of reduced major axis (RMA) regression (Equation 1: ln $Y = \ln F + f \ln M$) for scaling of the shoot and root respiration, fresh mass, and surface area in relation to the whole-plant fresh mass for each provenance using the data of plants within the weight range of 0.001 kg–0.1 kg (figure 2.7*a–f*).

Dependent variable	Provenance	*n*	Range of whole-plant fresh mass (kg)	Slope	95%CI of slope	Intercept	95%CI of intercept	R^2
Respiration rate								
Shoot (figure 2.7*a*)	Iwate	10	0.00106–0.0428	0.970	0.753–1.11	0.577	0.225–1.08	0.936
	Kochi	14	0.00121–0.058	0.984	0.789–1.11	0.618	0.207–1.15	0.934
	Nagano	19	0.00141–0.0157	1.240	0.715–1.57	2.180	0.136–14.8	0.661
	Shizuoka	8	0.00273–0.0767	0.912	0.73–1.09	0.413	0.166–0.76	0.950
	Yamagata	96	0.00103–0.07	0.936	0.849–1.01	0.434	0.251–0.661	0.767
Root (figure 2.7*d*)	Iwate	10	0.00106–0.0428	0.869	0.502–1.2	0.111	0.0234–0.482	0.776
	Kochi	14	0.00121–0.058	0.749	0.655–0.814	0.167	0.1–0.223	0.965
	Nagano	19	0.00141–0.0157	0.708	0.557–0.853	0.104	0.0468–0.23	0.779
	Shizuoka	8	0.00273–0.0767	0.801	0.567–0.916	0.185	0.0832–0.309	0.946
	Yamagata	96	0.00103–0.07	0.750	0.665–0.822	0.134	0.0794–0.207	0.859
Fresh mass								
Shoot (figure 2.7*b*)	Iwate	10	0.00106–0.0428	1.010	0.961–1.09	0.631	0.47–1	0.991
	Kochi	14	0.00121–0.058	1.020	0.947–1.06	0.403	0.264–0.5	0.990
	Nagano	19	0.00141–0.0157	1.170	1.09–1.27	1.030	0.689–1.78	0.980

	Shizuoka	8	0.00273–0.0767	1.070	0.862–1.22	0.439	0.21–0.943	0.984
	Yamagata	136	0.00103–0.07	0.943	0.884–1.01	0.281	0.195–0.432	0.913
Root (figure 2.7*e*)	Iwate	10	0.00106–0.0428	0.977	0.864–1.06	0.353	0.186–0.575	0.982
	Kochi	14	0.00121–0.058	0.995	0.972–1.03	0.612	0.54–0.755	0.995
	Nagano	19	0.00141–0.0157	0.891	0.811–0.955	0.323	0.207–0.456	0.979
	Shizuoka	8	0.00273–0.0767	0.969	0.922–1.07	0.581	0.458–0.868	0.994
	Yamagata	136	0.00103–0.07	1.070	1.02–1.12	0.897	0.64–1.22	0.963
Surface area								
Shoot (figure 2.7*c*)	Iwate	0						
	Kochi	9	0.00121–0.058	0.804	0.407–0.834	0.481	0.0398–0.541	0.989
	Nagano	0						
	Shizuoka	7	0.00273–0.0767	0.875	0.743–0.947	0.750	0.474–1.02	0.985
	Yamagata	86	0.00103–0.07	0.757	0.671–0.863	0.512	0.303–0.98	0.871
Root (figure 2.7*f*)	Iwate	0						
	Kochi	12	0.00121–0.058	0.595	0.534–0.812	0.569	0.406–2.19	0.920
	Nagano	0						
	Shizuoka	5	0.00273–0.0767	0.779	0.613–0.898	1.080	0.425–1.57	0.985
	Yamagata	85	0.00103–0.07	0.942	0.795–1.06	2.920	1.2–5.93	0.845

(v) Ontogenetic shift in the root fraction of the whole plant

Using the obtained functions for the relationships between shoot and root to whole-plant fresh mass shown in figures 2.6*a–c*, we calculated the root fraction (root/whole plant, %) from seedlings to mature trees, as shown in figure 2.8. Overall, the root fraction significantly increased in small seedlings and gradually decreased in larger plants with increasing plant size. Calculated at 10 mg intervals, the peak of root fraction was 47.8% at 0.00274 kg for respiration rate, 64.3% at 0.00436 kg for fresh mass, and 78.2% at 0.00458 kg for surface area. These results indicate that the allocation of metabolic products is preferred for roots during the early growth stage, and gradually shifts to for shoots in mature trees.

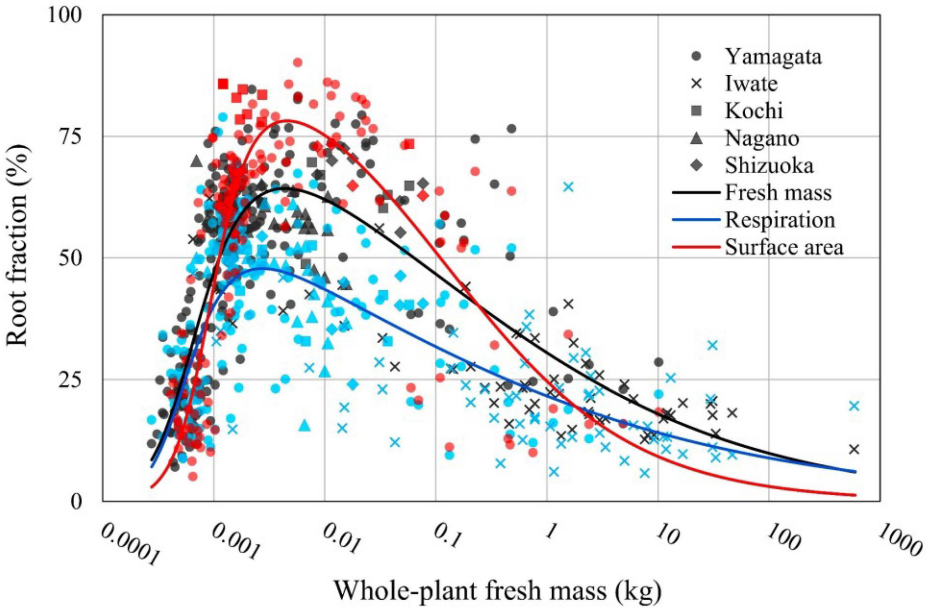

Figure 2.8 Plot diagram of the root fraction (%) of respiration rates, fresh mass, and surface area *F. crenata* in relation to whole-plant fresh mass from germination to mature tree stages. Black, fresh mass; red, surface area; blue, respiration rates. Different symbols represent five different provenances in Japan.

4. Discussion

A convex upward trend was observed for the whole-plant respiration of *F. crenata*, with the scaling exponent gradually decreasing from over 3.0 during seed germination to approximately 0.75 in mature trees (red line in figure 2.3*a*). This means that Kleiber's 3/4 power law [11] is not followed by the plants in the early growth stage, from seed germination to before the main leaves develop, but it is followed by the plants with main leaves from the seedling stage to the mature tree stage. In the initial growth stage from seed germination to before expansion of true leaves, plants do not have developed photosynthetic performance yet. For such an initial growth stage, Huang et al. (2020) [40] reported a steep increase in mass-specific respiration after a water-triggered break of seed dormancy and strong constraints by water content on the respiration rate. Therefore, it is likely that the high scaling exponents for the early growth stage with undeveloped plant form is likely caused by the strong constraint by water content. The convex upward trend was consistent with our previous study on the interspecific scaling of whole-plant respiration with the exponent shifting from approximately 1.0 in the seedling to 0.75 in the giant tree [15]. Therefore, our results suggest that the exponent of 0.75 is shown in the range of body size from seedling to mature trees that have structure and function of carbon gain and water uptake.

Interestingly, respiration rates, fresh mass, and surface area of whole plants, shoots, and roots seem to considerably converge along their sizes, even though the dataset included trees from various provenances different in climatic conditions. Statistical analysis confirmed that there was no difference in the respiration of whole seedling plants among the provenances (figure 2.3*b*). Similarly, there were no noticeable differences among the provenances were found in the scaling of shoots and roots (in respiration, fresh mass, and surface area) with body size, as indicated in figure 2.6 and figure 2.7. This suggests that, despite the intraspecific variation in single-leaf level morphology and physiology [29,30] and gene phylogeny [28], variation in the structure and

function of entire shoot and root is limited to a certain range according to plant size during ontogeny, consistent with Mori et al. (2010) [15]. This is possibly because zero-sum dynamics between shoot and root in energy use is subjected to physicochemical constraints that are general for environments and phylogenies. This size-dependent energy balance between shoot and root may form a universal baseline of whole-plant respiration, which may be a physiological background of Kleiber's law [11] and the WBE model [12] for terrestrial plants.

Consistent with previous empirical studies [15,41], the scaling of shoot respiration to shoot fresh mass (figure 2.5*a*) showed negative allometry, likely due to the accumulation of inactive tissue through ontogeny. The convex downward trend in root respiration with root fresh mass (figure 2.5*a*) was unexpected. Considering the comparatively small sample size of mature trees, further measurements are needed to confirm the robustness of this result. However, it seems certain that roots tend to have lower mass-specific respiration than shoots in a wide range of fresh mass values from seedlings to mature trees. Furthermore, within small sizes, the scaling of root surface area to root mass indicated the exponent > 1.0 (figure 2.4*b*), resulting in relatively clear convex downward trend in root respiration with root surface area (figure 2.5*b*). Furthermore, the relationships between respiration and fresh mass of the whole plant (black line in figure 2.3*a*) showed a similar trend to that of roots (convex downward), rather than the shoots (linear). This emphasises the importance of root development for tree growth in the course of ontogeny.

In the range of body size from seedlings to mature trees, whole-plant respiration with whole-plant fresh mass was well expressed even as relatively stable allometry. In contrast, shoot and root (in respiration, fresh mass, and surface area) showed contrasting and clear convex trends according to body size on the log-log coordinates, convex downward and convex upward curves, respectively (figures 2.6*a–c*). Furthermore, their asymptotes' intersection point P was found to be smaller than 0.002 kg. This suggests that the metabolic product in plants is preferentially invested

in roots during the early growth stage immediately after germination, and subsequently for shoots at later stages up to mature trees (figure 2.8). During the early growth stage, the root fraction increased significantly up to 78.2% in surface area, and only to 47.8% in respiration, indicating that root growth during the early growth stage is rapid and energetically efficient [19]. In the size below 0.002 kg, we also observed that shoot respiration, fresh mass, and surface area decreased with increasing plant size, as shown by the exponent < 0 in figures 2.6*a–c*. This may be due to the decrease in cotyledons (seed reserves), which are the main energy source for small seedlings whose photosynthetic capacity has not yet been fully developed [42,43]. Conversely, the subsequent preferential increase in shoots suggests an increase in photosynthetic capacity. This shift is consistent with the general perception of the tree growth model that the increase in body size, i.e., dry mass, is relatively small in the early growth phase and growth is enhanced later [44]. Therefore, our results indicate that the initial slow growth stage is characterised by preferential root growth to accelerate photosynthetic performance and subsequent shoot growth.

It has been widely recognised that the entire plant growth is expressed as sigmoid curves, in which the initial growth rate is low, subsequently exponentially increases, and finally declines toward asymptote [45]. However, the physiological mechanisms that cause the decline in growth with increasing size after the mature growth stage have not been fully elucidated and remain controversial [44]. We measured trees up to the mature and large size at which individual growth of *F. crenata* would begin to decline [46,47] and observed that roots asymptote before the shoot (figures 2.6*a–c*). This suggests that the decline in root growth during the mature stage causes an imbalance between water uptake and carbon acquisition, and consequently reduces shoot and whole-plant growth. Therefore, it is probable that the sigmoidal growth curve is likely to be a consequence of the ontogenetic transition of the root:shoot ratio, and that the entire course of whole-plant growth is largely regulated by root growth. In summary, it is expected that the whole-

plant structure and function ontogenetically shift to be efficient and preferential for water acquisition during the early growth stage and carbon acquisition in mature trees. Elucidating the capacity for water uptake and carbon acquisition at the individual level from seedlings to mature trees will be a future challenge. These results will also help to elucidate the underlying mechanisms that constrain the chronological changes in the CO_2 budget of forests, including roots.

References

1. Thornley JHM. 1972 A balanced quantitative model for root: shoot ratios in vegetative plants. *Ann. Bot.* **36**, 431–441.
2. McCarthy MC, Enquist BJ. 2007 Consistency between an allometric approach and optimal partitioning theory in global patterns of plant biomass allocation. *Funct. Ecol.* **21**, 713–720.
3. Bloom AJ, Chapin FS, Mooney HA. 1985 Resource limitation in plants resource limitation in plants – an economic analogy. *Annu. Rev. Ecol. Syst.* **16**, 363–392.
4. Gedroc JJ, McConnaughay KDM, Coleman JS. 1996 Plasticity in root/shoot partitioning: optimal, ontogenetic, or both? *Funct. Ecol.* **10**, 44–50.
5. Müller I, Schmid B, Weiner J. 2000 The effect of nutrient availability on biomass allocation patterns in 27 species of herbaceous plants. *Perspect. Plant Ecol. Evol. Syst.* **3**, 115–127.
6. Poorter H *et al.* 2015 How does biomass distribution change with size and differ among species? An analysis for 1200 plant species from five continents. *New Phytol.* **208**, 736–749.
7. Ledo A *et al.* 2018 Tree size and climatic water deficit control root to shoot ratio in individual trees globally. *New Phytol.* **217**, 8–11.
8. Enquist BJ, Niklas KJ. 2002 Global allocation rules for patterns of biomass partitioning in seed plants. *Science* **295**, 1517–1520.
9. Sibly RM, Brown JH, Kodric-Brown A. 2012 *Metabolic ecology: a scaling approach*. John Wiley& Sons, Chichester.
10. O'Leary BM, Asao S, Millar AH, Atkin OK. 2019 Core principles which explain variation in respiration across biological scales. *New Phytol.* **222**, 670–686.
11. Kleiber M. 1932 Body size and metabolism. *Hilgardia* **6**, 315–353.
12. West GB, Brown JH, Enquist BJ. 1997 A general model for the origin of allometric scaling laws in biology. *Science.* **276**, 122–126.
13. Makarieva AM, Gorshkov VG, Li BL, Chown SL, Reich PB, Gavrilov VM. 2008 Mean mass-specific metabolic rates are strikingly similar across life's major domains: Evidence for life's metabolic optimum. *Proc. Natl. Acad. Sci. USA.* **105**, 16994–16999.
14. Banavar JR, Cooke TJ, Rinaldo A, Maritan A. 2014 Form, function, and evolution of living organisms. *Proc. Natl. Acad. Sci. USA.* **111**, 3332–3337.

15. Mori S *et al.* 2010 Mixed-power scaling of whole-plant respiration from seedlings to giant trees. *Proc. Natl. Acad. Sci. USA.* **107**, 1447–1451.

16. Atkin O. 2010 Recommendation of [Mori S et al. at *Proc. Natl. Acad. Sci. USA*. 2010, **107**, 1447–1451]. In F1000Prime

17. Ballesteros FJ, Luque B. 2018 Gravity and life. In *Habitability of the universe before earth* (eds R Gordon & A Sharov), Vol. 1, pp. 3–26. Academic Press, Cambridge

18. Wang M, Mori S, Kurosawa Y, Ferrio JP, Yamaji K, Koyama K. 2021 Consistent scaling of whole-shoot respiration between Moso bamboo (*Phyllostachys pubescens*) and trees. *J. Plant Res.* **134**, 989–997.

19. Kurosawa Y, Mori S, Wang M, Ferrio JP, Yamaji K, Koyama K, Haruma T, Doyama K. 2021 Initial burst of root development with decreasing respiratory carbon cost in *Fagus crenata* Blume seedlings. *Plant Species Biol.* **36**, 146–156.

20. Levin SA. 1992 The problem of pattern and scale in ecology: The Robert H. MacArthur award lecture *Ecology* **73**, 1943–1967.

21. Levin SA. 1999 *Fragile dominion: complexity and the commons*. Perseus Books. Reading.

22. Chave J. 2013 The problem of pattern and scale in ecology: What have we learned in 20 years? *Ecol. Lett.* **16**, 4–16.

23. Weigelt A *et al.* 2021 An integrated framework of plant form and function: the belowground perspective. *New Phytol.* **232**, 42–59.

24. Raven JA, Edwards D. 2017 Roots: evolutionary origins and biogeochemical significance. *J. Exp. Bot.* **52**, 381–401.

25. Mori S, Hagihara A. 1988 Respiration in stems of hinoki (*Chamaecyparis obtusa*) trees. *J. Japanese For. Soc.* **70**, 187–481.

26. Mori S, Hagihara A. 1991 Root respiration in *Chamaecyparis obtusa* trees. *Tree Physiol*. **8**, 217–225.

27. Reich PB, Tjoelker MG, Machado JL, Oleksyn J. 2006 Universal scaling of respiratory metabolism, size and nitrogen in plants. *Nature* **439**, 457–461.

28. Fujii N, Tomaru N, Okuyama K, Koike T, Mikami T, Ueda K. 2002 Chloroplast DNA phylogeography of *Fagus crenata* (Fagaceae) in Japan. *Plant Syst. Evol.* **232**, 21–33.

29. Bayramzadeh V, Funada R, Kubo T. 2008 Relationships between vessel element anatomy and physiological as well as morphological traits of leaves in *Fagus crenata* seedlings originating from different provenances. *Trees.* **22**, 217–224.

30. Tateishi M, Kumagai T, Suyama Y, Hiura T. 2010 Differences in transpiration characteristics of Japanese beech trees, *Fagus crenata*, in Japan. *Tree Physiol.* **30**, 748–760.

31. Ferrio JP, Kurosawa Y, Wang M, Mori S. 2018 Hydraulic constraints to whole-tree water use and respiration in young *Cryptomeria* trees under competition. *Forests* **9**, 449.

32. Gillooly JF, Brown JH, West GB, Savage VM, Charnov EL. 2001 Effects of size and temperature on metabolic rate effects of size and temperature on metabolic rate. *Science.* **293**, 2248–2251.

33. Whittaker RH, Woodwell GM. 1967 Surface area relations of woody plants and forest communities. **54**, 931–939.

34. Shinozaki, K. (1979). Summation of simple power functions. *Chem. Biol.* **17**, 331–333.

35. Elzhov TV, Mullen KM, Spiess AN, Bolker B. 2013 minpack.lm: R interface to the Levenberg–Marquardt nonlinear least-squares algorithm found in MINPACK, plus support for bounds.

36. R Core Team. 2019 *R: a language and environment for statistical computing*. Vienna, Austria: R Foundation for Statistical Computing.

37. Burnham KP, Andersen DR 2002 *Model selection and multimodel inference: a practical information—theoretical Approach*. Springer, New York

38. Niklas KJ, Hammond ST. 2014 Assessing Scaling Relationships: Uses, Abuses, and Alternatives. *Int. J. Plant Sci.* **175**, 754–763.

39. Hammer Ø, Harper DAT, Ryan PD. 2001 Past: Paleontological statistics software package for education and data analysis. *Palaeontol. Electron.* **4**, 1–9.

40. Huang H *et al.* 2020 A general model for seed and seedling respiratory metabolism. *Am. Nat.* **195**, 534–546.

41. Huang H *et al.* 2020 Water content quantitatively affects metabolic rates over the course of plant ontogeny. *New Phytol.* **228**, 1524–1534.

42. Kitajima K. 2002 Do shade-tolerant tropical tree seedlings depend longer on seed reserves? Functional growth analysis of three Bignoniaceae species. *Funct. Ecol.* **16**, 433–444.

43. Ampofo ST, Moore KG, Lovell PH. 1976 The role of the cotyledons in four *Acer* species and in *Fagus sylvatica* during early seedling development. *New Phytol.* **76**, 31–39.

44. Weiner J, Thomas SC. 2001 The nature of tree growth and the "age-related decline in forest productivity". *Oikos* **94**, 374–376.

45. Tjørve E, Tjørve KMC. 2010 A unified approach to the Richards-model family for use in growth analyses: Why we need only two model forms. *J. Theor. Biol.* **267**, 417–425.

46. Ono K, Yasuda Y, Matsuo T, Hoshino D, Chiba Y, Mori S. 2013 Estimating forest biomass using allometric model in a cool-temperate *Fagus crenata* forest in the Appi highlands, Iwate, Japan. *Bull. For. For. Prod. Res. Inst.* **12**, 125–141.

47. Bourque CPA, Bayat M, Zhang C. 2019 An assessment of height–diameter growth variation in an unmanaged *Fagus orientalis*-dominated forest. *Eur. J. For. Res.* **138**, 607–621.

Acknowledgement

First and foremost, I would like to express my gratitude to my supervisor, Prof. Shigeta Mori. He has given me continuous and appropriate support in all aspects of my academic research and daily life during my PhD. This PhD thesis could not have been completed without his efforts.

I would also like to thank my associate supervisors, Prof. Shunichi Kikuchi and Prof. Shinji Akada, for their helpful comments and discussions on my thesis.

I would like to thank my collaborators Prof. Juan pedro ferrio, Prof. Keiko Yamaji, Prof. Kohei Koyama, Prof. Shingo Tomiyama, Dr. Toshikatsu Haruma, and Dr. Kohei Doyama for their helpful comments on my work from their respective fields of expertise. I am also deeply indebted to another collaborator, Dr. Tomohiro Nishizono, for his considerable assistance with the data analysis. I am very grateful to them for their great contributions to my research.

I would also like to express my gratitude to Prof. Atsushi Ishida and Prof. Kikukatsu Ito for their valuable comments and suggestions on my work. I am also grateful to the staff of the Yamagata University Experimental Forest, Daisuke Arai and Sadaaki Iizuka, for their support during our fieldwork. Many thanks to Prof. Atsuhiro Iio and Prof. Tomoaki Ichie for offering us with beech seeds.

I would like to thank my colleagues in the laboratory for their support with my field measurements and daily support.

Finally, I would like to express my grateful thanks to the professors and staffs of the United Graduate School of Agricultural Sciences, Iwate University and the Faculty of Agriculture of Yamagata University who extended me their kind assistance.

List of Publications

Original papers

1. Kurosawa Y, Mori S, Wang M, Ferrio JP, Yamaji K, Koyama K, Haruma T, Doyama K. 2021 Initial burst of root development with decreasing respiratory carbon cost in *Fagus crenata* Blume seedlings. *Plant Species Biol*. **36**, 146–156. (Chapter 1)
2. Kurosawa Y, Wang M, Mori S, Haruma T, Noji K, Doyama K, Yamaji K, Tomiyama S. 2021 Evaluation of initial growth and respiration of various plants for revegetation of dumping sites in closed mine. *Resour. Process*. **67**. 122–127. (in Japanese)

Related papers

1. Ferrio JP, Kurosawa Y, Wang M, Mori S. 2018 Hydraulic constraints to whole-tree water use and respiration in young *Cryptomeria* trees under competition. *Forests* **9**, 449.
2. Kattge J, Bönisch G, Díaz S, Lavorel S, …, Kurosawa Y, …, et al. 2020 TRY plant trait database – enhanced coverage and open access. *Glob. Chang. Biol.* **26**, 119–188.
3. Wang M, Mori S, Kurosawa Y, Ferrio JP, Yamaji K, Koyama K. 2021 Consistent scaling of whole-shoot respiration between Moso bamboo (*Phyllostachys pubescens*) and trees. *J. Plant Res.* **134**, 989–997.
4. Doyama K, Yamaji K, Haruma T, Ishida A, Mori S, Kurosawa Y. 2021 Zn tolerance in the evergreen shrub, *Aucuba japonica*, naturally growing at a mine site: Cell wall immobilization, aucubin production, and Zn adsorption on fungal mycelia. *PLOS ONE* **16**, e0257690.